

**Magnetic Properties of a Diferrous-Water Complex and Ligands for  
Modeling the Active Site of MMOH**

by

Amy E. Kelly

B.S., Chemistry and Geochemistry

Caltech, 2002

SUBMITTED TO THE DEPARTMENT OF CHEMISTRY IN PARTIAL FULFILLMENT  
OF THE REQUIREMENTS FOR THE DEGREE OF

MASTERS IN INORGANIC CHEMISTRY  
AT THE  
MASSACHUSETTS INSTITUTE OF TECHNOLOGY

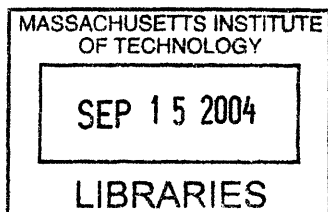
September 2004

© Massachusetts Institute of Technology, 2004  
All rights reserved

Signature of Author: \_\_\_\_\_  
Department of Chemistry  
August 30, 2004

Certified by: \_\_\_\_\_  
Stephen J. Lippard  
Arthur Amos Noyes Professor of Chemistry  
Thesis Supervisor

Accepted by: \_\_\_\_\_  
Robert W. Field  
Chairman, Departmental Committee on Graduate Students



ARCHIVES

# Magnetic Properties of a Diferrous-Water Complex and Ligands for Modeling the Active Site of MMOH

by

Amy E. Kelly

Submitted to the Department of Chemistry on August 30, 2004, in partial fulfillment of the requirements for the degree of Masters.

## Abstract

### Chapter 1. The Importance of Modeling Diiron Sites in Nature

There are a variety of metalloenzymes that have nearly identical carboxylate-bridged diiron active sites. An example is sMMOH, an enzyme that catalyzes the conversion of methane to methanol. A detailed description of the active site of sMMOH<sub>red</sub> is given and attempts at reproducing its structure in a model complex are discussed.

### Chapter 2. A Diiron(II) Diaqua Complex: Modeling Water in the Active Site of sMMOH<sub>red</sub>

There are water molecules in the first and second coordination spheres of the diiron centers in sMMOH<sub>red</sub>. A carboxylate-bridged diferrous complex,  $[\text{Fe}_2(\mu\text{-O}_2\text{CAr}^{\text{Tol}})_2(\mu\text{-OH}_2)_2(\text{O}_2\text{CAr}^{\text{Tol}})_2(\text{THF})_2]$ , was synthesized to incorporate the presence of water in a model complex and to investigate the function(s) of these water molecules. The synthesis, structural characterization and magnetic properties of this complex are presented.

### **Chapter 3. Ligands for Modeling the Syn Disposition of Nitrogen Atoms in the Active Site of MMOH**

The active sites of a variety of carboxylate-bridged diiron metalloenzymes are very similar and feature the syn disposition of two histidine ligands with respect to the iron-iron vector. This orientation has not yet been modeled in a diiron complex with four carboxylate ligands and a stable yet flexible platform. Such geometry may be necessary to replicate the functions of these enzymes. The syntheses of ligands intended to enforce this syn disposition are described and directions for future ligand design are outlined.

Thesis Supervisor: Stephen J. Lippard

Title: Department Head and Arthur Amos Noyes Professor of Chemistry

*To those who believe in me*

## Acknowledgements

The Chemistry Department has been good to me. I have made many friends and learned a lot about Chemistry and especially about life. I am grateful to Steve for giving me this opportunity, and to the rest of the faculty for augmenting my education. I must also thank Jane Kuzelka, Sungho Yoon, Jeremy Kodanko, Emily Carson, Edit Tshuva, Sumitra Mukhopadhyay, and Rayane Moreira for teaching and encouraging me, helping me feel at home here, and making me laugh. Though not directly involved in my project I would like to thank Mi Hee Lim and Leslie Murray for their constant support and friendship.

Most importantly, I must thank my loved ones. My utmost appreciation goes to my parents for always being there for me, my grandfather for sparking my love of science at a young age, and Shane Mauss for standing by my side in hardship.

Lastly, I would just like to thank all of the people that believed in me and helped me along my journey. All of the Chemistry and Geology faculty at Caltech, especially Harry Gray and George Rossman, and the professors I did research for in the summers, Don Berry at the University of Pennsylvania and Eric Wenger and Martin Bennett at the Australian National University. They were all an important part of my life as both mentors and friends.

This work was supported by a grant from the National Institute of General Medical Sciences. I would like to thank Dr. Sungho Yoon for all of his indispensable advice and guidance, helping me operate the Mössbauer and SQUID susceptometer and teaching me the programs used to analyze the data obtained. I would like to thank Dr. Jeremy Kodanko for his help with organic syntheses and Mrs. Emily Carson for aid using the 500 MHz spectrometer.

<b>Table of Contents</b>	
Abstract.....	2
Dedication.....	4
Acknowledgements.....	5
Table of Contents.....	6
List of Tables.....	8
List of Schemes.....	9
List of Figures.....	10
<b>Chapter 1. The Importance of Modeling Diiron Sites in Nature.....</b>	<b>12</b>
Perspectives and Implications for Future Work.....	13
References.....	16
<b>Chapter 2. A Diiron(II) Diaqua Complex: Modeling Water in the Active Site of</b>	
<b>sMMO<sub>red</sub>.....</b>	<b>21</b>
Introduction.....	22
Experimental Section.....	23
General Procedures.....	23
Synthetic Procedures.....	23
X-ray Crystallography.....	24
<sup>57</sup> Fe Mössbauer Spectroscopy.....	24
SQUID Susceptometry.....	25
Results and Discussion.....	26
Synthesis of [Fe <sub>2</sub> (μ-O <sub>2</sub> CAr <sup>Tol</sup> ) <sub>2</sub> (μ-OH <sub>2</sub> ) <sub>2</sub> (O <sub>2</sub> CAr <sup>Tol</sup> ) <sub>2</sub> (THF) <sub>2</sub> ] (1).....	26
Structural Characterization.....	26
Mössbauer Spectroscopic Properties.....	28
Magnetic Properties.....	29
Summary and Conclusions.....	31
References and Notes.....	33
<b>Chapter 3. Ligands for Modeling the Syn Disposition of Nitrogen Atoms in the</b>	
<b>Active Site of MMOH.....</b>	<b>47</b>
Introduction.....	48

Experimental Section.....	51
General Procedures.....	51
Synthetic Procedures.....	51
Physical Measurements.....	55
Results and Discussion.....	55
Attempts at Incorporating Isopropyl Groups in the BCQEB Design.....	55
Synthesis of 3-Isopropylphenylamine ( <b>1a</b> ).....	56
Synthesis of N-(3-Isopropylphenyl)-2,2-dimethylpropionamide ( <b>1b</b> ) .....	57
Synthesis of 2- <i>tert</i> -Butoxycarbonylamino-6-chlorobenzoic Acid ( <b>2a</b> ) and 2- <i>tert</i> - Butoxycarbonylamino-6-chlorobenzoic Acid Methyl Ester ( <b>2b</b> ).....	57
Design and Synthesis of Silanes ( <b>3a – 3d</b> ).....	57
Synthesis of 4,6-Dibenzofuranbis(isoquinoline) ( <b>4</b> ) and Attempts at Metallation.....	58
Conclusions and Implications for Future Work.....	59
References.....	61
<b>Biographical Note</b> .....	<b>75</b>

**List of Tables****Chapter 2**

Table 2.1.	Summary of X-ray crystallographic information.....	37
Table 2.2.	Selected bond lengths (Å) and angles (deg) for <b>1A</b> and <b>1B</b> .....	38
Table 2.3.	Summary of Mössbauer parameters recorded at 4.2 K (mm s <sup>-1</sup> ).....	39
Table 2.4.	SQUID data.....	40



**List of Schemes****Chapter 3**

Scheme 3.1. Proposed synthesis of 2-amino-6-isopropylbenzoic acid.....	64
Scheme 3.2. Proposed synthesis of BICQEB <sup>R</sup> , derived from the successful synthesis of BCQEB <sup>R</sup> .....	65
Scheme 3.3. Synthesis of 4,6-dibenzofuranbis(isoquinoline) .....	66
Scheme 3.4. Proposed synthesis of 7-isopropyl-quinoline-8-carboxylic acid methyl ester.....	67

## List of Figures

### Chapter 1

- Figure 1.1. Representations of the active sites of sMMOH<sub>red</sub>, RNR-R2 and the reduced form of Δ<sup>9</sup>D..... 18
- Figure 1.2. Detailed representation of the active site of sMMOH<sub>red</sub>..... 19
- Figure 1.3. Schematic representation of an example of a sterically hindered carboxylic acid, 2,6-di(*p*-tolyl)benzoic acid (Ar<sup>Tol</sup>CO<sub>2</sub>H).....20

### Chapter 2

- Figure 2.1. Detailed representation of the active site of sMMOH<sub>red</sub>..... 41
- Figure 2.2. ORTEP diagrams of **1**, both the core and asymmetric unit, showing 50 % probability thermal ellipsoids..... 42
- Figure 2.3. Zero-field Mössbauer spectrum recorded at 4.2 K of a solid sample.....43
- Figure 2.4. SQUID spectra. A plot of μ<sub>eff</sub> vs. T for all 5 samples run. A plot of χ vs. T and μ<sub>eff</sub> vs. T for sample 3, a representative sample..... 44
- Figure 2.5. FT-IR spectrum of [Fe<sub>2</sub>(μ-O<sub>2</sub>CAr<sup>Tol</sup>)<sub>2</sub>(μ-OH)<sub>2</sub>(O<sub>2</sub>CAr<sup>Tol</sup>)<sub>2</sub>(THF)<sub>2</sub>]..... 45
- Figure 2.6. Figure displaying the difference in THF orientation between the monoclinic and orthorhombic crystal structures..... 46

### Chapter 3

- Figure 3.1. Detailed representation of the active site of sMMOH<sub>red</sub>..... 68
- Figure 3.2. Proposed catalytic reaction cycle with only spectroscopically visible species.....69
- Figure 3.3. Example of a sterically hindered carboxylic acid, 2,6-di(*p*-tolyl)benzoic acid (Ar<sup>Tol</sup>CO<sub>2</sub>H)..... 70
- Figure 3.4. Representation of BQEB.....71
- Figure 3.5. Representation of H<sub>2</sub>BCQEB.....72
- Figure 3.6. Desired final diferrous product..... 73

Figure 3.7. General representation of synthesized silanes..... 74

**Chapter 1**  
**The Importance of Modeling Diiron Sites in Nature**

---

## Perspectives and Implications for Future Work

Modeling enzymes is important to bioinorganic chemistry. Such studies have helped in protein structure analysis, which is more complex in the natural system. Methanotrophic bacteria catalyze the oxygenation of methane to methanol.<sup>1,2</sup> The strain *Methylococcus capsulatus* (Bath) has an enzyme, soluble methane monooxygenase (sMMO), that is responsible for this conversion. If this reaction could be replicated by a small molecule catalyst, then natural gas might be more easily shipped as a liquid with significant industrial value. In addition, the active site of the hydroxylase component of sMMO (sMMOH) is homologous to those of the R2-subunit of ribonucleotide reductase (RNR-R2)<sup>3</sup> and  $\Delta$ -9 desaturase ( $\Delta^9$ D).<sup>4</sup> Thus, a better understanding of how the diiron site of MMOH functions may help us understand these other enzymes as well. The active sites of the reduced form of sMMOH (sMMOH<sub>red</sub>), RNR-R2, and the reduced form of  $\Delta^9$ D are shown in Figure 1.1. Each has a diferrous center comprising four carboxylates and two histidines that are located on the same side of the iron-iron vector.

The structure of sMMOH<sub>red</sub> is depicted schematically in Figure 1.2. There has been much progress in modeling this structure and a number of complexes have been synthesized that have the proper ligand stoichiometry.<sup>5-9</sup> Significant challenges remain, however, such as reproducing the syn disposition of the nitrogen donors and the presence of water in the active site.

One of the biggest challenges in preparing such a small molecule model complex is the absence of the polypeptide backbone, which maintains the structural integrity of the active site,<sup>10</sup> creates a hydrophobic pocket,<sup>2</sup> and performs other roles that are

difficult to duplicate.<sup>11-15</sup> A major breakthrough in the lab was the employment of sterically hindered terphenyl-based carboxylates, such as 2,6-di(*p*-tolyl)benzoate ( $\text{Ar}^{\text{Tot}}\text{CO}_2^-$ ) (Figure 1.3). Some previous modeling attempts had difficulty in maintaining dinuclear transition states during oxygenation reactions.<sup>11,15</sup> The  $\text{Ar}^{\text{Tot}}\text{CO}_2^-$  carboxylate has sufficient steric bulk to facilitate the synthesis of complexes with a dimetallic core and avoid such bimolecular decay.<sup>3,11,16-17</sup> Complexes employing this ligand were then synthesized comprising four carboxylate ligands and two nitrogen donors bound to the diiron center. Although this stoichiometry is the desired one, during the self-assembly process, the nitrogen donors were always positioned anti to each other in the product.<sup>5-9</sup> It is necessary for the N-donors to have syn stereochemistry to model properly the active sites of the enzyme. This difference may allow for a better match to the electronic properties of sMMOH, as well as reproduce the reactivity with dioxygen and the oxidation of hydrocarbons.<sup>18</sup> There have been a few prior attempts to enforce the syn geometry of the nitrogen donors, mainly by using a diethynylbenzene backbone.<sup>19</sup> However, a diferrous complex with four carboxylates and two nitrogen donors located syn to one another has only been synthesized with an XDK<sup>20</sup> or phthalazine<sup>19</sup> framework. The XDK platform is too restrictive to allow a Q type intermediate to form. The phthalazine backbone positions the nitrogen atoms much too close to each other to mimic the active site structurally, and the complex does not maintain its dinuclearity upon oxidation. A complex is needed that is diferrous, has four carboxylate ligands, two nitrogen donors with a syn disposition, and a platform that is stable enough to maintain dinuclearity, but flexible enough to let a Q type intermediate form.

Another aspect of the enzyme active site structures that has not been adequately modeled is the presence of coordinated water. There have been a few diferrous aqua complexes synthesized previously,<sup>10,21-24</sup> but it was not until recently that they have been thoroughly examined.<sup>25</sup>

My goals have been to create new ligands that will enforce the syn disposition of nitrogen donors, both using the diethynylbenzene backbone and newly designed silane and dibenzofuran platforms, as well as to study a new diaqua-bridged diferrous complex,  $[\text{Fe}_2(\mu\text{-O}_2\text{CAr}^{\text{Tol}})_2(\mu\text{-OH}_2)_2(\text{O}_2\text{CAr}^{\text{Tol}})_2(\text{THF})_2]$ . Progress towards achieving these goals, which will lead to the synthesis of more structurally accurate model complexes for the diiron site in  $\text{sMMOH}_{\text{red}}$ , is the subject of this thesis.

**References**

1. Du Bois, J.; Mizoguchi, T. J.; Lippard, S. J. *Coord. Chem. Rev.* **2000**, *200–202*, 443–485.
2. Merkx, M.; Kopp, D. A.; Sazinsky, M. H.; Blazyk, J. L.; Müller, J.; Lippard, S. J. *Angew. Chem. Int. Ed.* **2001**, *40*, 2782–2807.
3. Feig, A. L.; Lippard, S. J. *Chem. Rev.* **1994**, *94*, 759–805.
4. Yang, Y.-S.; Broadwater, J. A.; Pulver, S. C.; Fox, B. G.; Solomon, E. I. *J. Am. Chem. Soc.* **1999**, *121*, 2770–2783.
5. Lee, D.; Lippard, S. J. *J. Am. Chem. Soc.* **2001**, *123*, 4611–4612.
6. Lee, D.; Hung, P.-L.; Spingler, B.; Lippard, S. J. *Inorg. Chem.* **2002**, *41*, 521–531.
7. Lee, D.; Lippard, S. J. *Inorg. Chem.* **2002**, *41*, 827–837.
8. Lee, D.; Pierce, B.; Krebs, C.; Hendrich, M. P.; Huynh, B. H.; Lippard, S. J. *J. Am. Chem. Soc.* **2002**, *124*, 3993–4007.
9. Lee, D.; Lippard, S. J. *Inorg. Chem.* **2002**, *41*, 2704–2719.
10. Reynolds, R. A., III.; Dunham, W. R.; Coucouvanis, D. *Inorg. Chem.* **1998**, *37*, 1232–1241.
11. Feig, A. L.; Masschelein, A.; Bakac, A.; Lippard, S. J. *J. Am. Chem. Soc.* **1997**, *119*, 334–342.
12. Whittington, D. A.; Lippard, S. J. *J. Am. Chem. Soc.* **2001**, *123*, 827–838.
13. Hagadorn, J. R.; Que, L., Jr.; Tolman, W. B. *Inorg. Chem.* **2000**, *39*, 6086–6090.
14. Broadwater, J. A.; Achim, C.; Münck, E.; Fox, B. G. *Biochemistry* **1999**, *38*, 12197–12204.



15. Feig, A. L.; Becker, M.; Schindler, S.; van Eldik, R.; Lippard, S. J. *Inorg. Chem.* **1996**, *35*, 2590–2601.
16. Tolman, W. B.; Que, L., Jr. *J. Chem. Soc., Dalton Trans.* **2002**, *5*, 653–660.
17. Kuzelka, J.; Spingler, B.; Lippard, S. J. *Inorg. Chim. Acta.* **2002**, *337*, 212–222.
18. Baik, M.-H.; Lippard, S. J. Unpublished results.
19. Kuzelka, J.; Farrell, J. R.; Lippard, S. J. *Inorg. Chem.* **2003**, *42*, 8652–8662.
20. LeCloux, D. D.; Barrios, A. M.; Mizoguchi, T. J.; Lippard, S. J. *J. Am. Chem. Soc.* **1998**, *120*, 9001–9014.
21. Hagen, K. S.; Lachicotte, R.; Kitaygorodskiy, A.; Elbouadili, A. *Angew. Chem. Int. Ed. Engl.* **1993**, *32*, 1321–1324.
22. Hagan, K. S.; Lachicotte, R. *J. Am. Chem. Soc.* **1992**, *114*, 8741–8742.
23. Hagan, K. S.; Lachicotte, R.; Kitaygorodskiy, A. *J. Am. Chem. Soc.* **1993**, *115*, 12617–12618.
24. Coucouvanis, D.; Reynolds, R. A., III.; Dunham, W. R. *J. Am. Chem. Soc.* **1995**, *117*, 7570–7571.
25. Yoon, S.; Kelly, A. E.; Lippard, S. J. *Polyhedron* **2004**, in press.

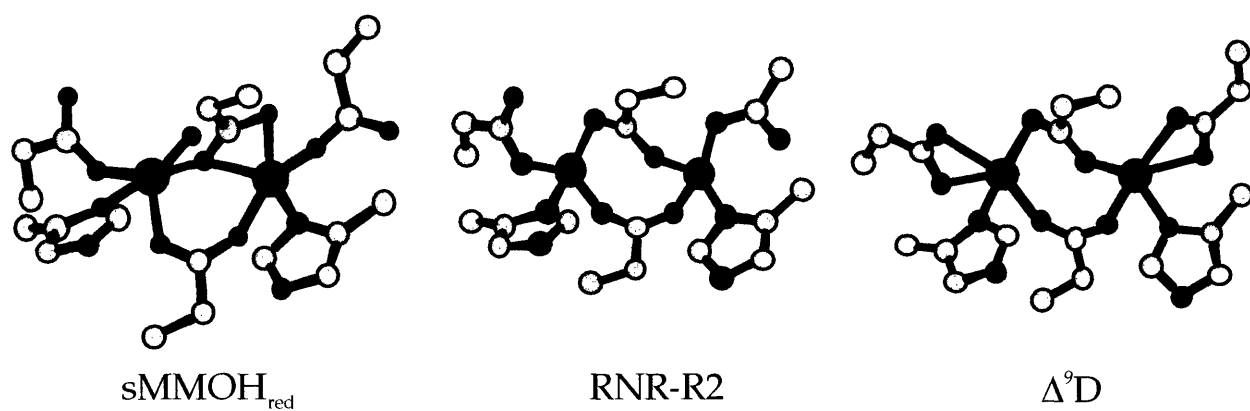


**Figure 1.1.** Representations of the active sites of sMMOH<sub>red</sub>, RNR-R2 and the reduced form of  $\Delta^9\text{D}$ . Figures used with permission from Lee, D.; Lippard, S. J. *Inorg. Chem.* **2002**, *41*, 2704–2719.

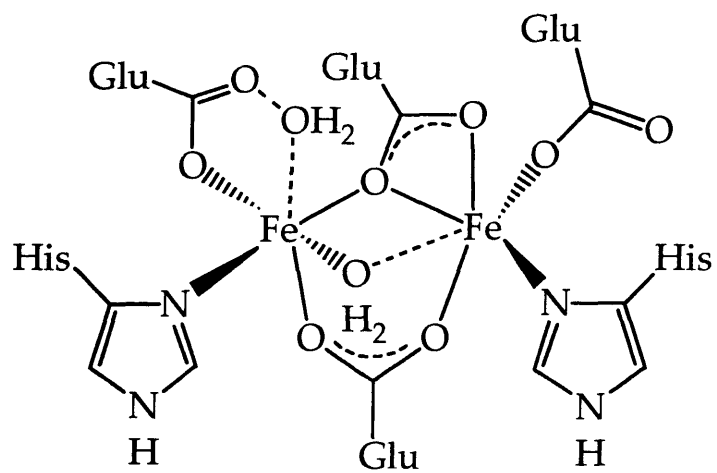


**Figure 1.2.** Detailed representation of the active site of sMMOH<sub>red</sub>.

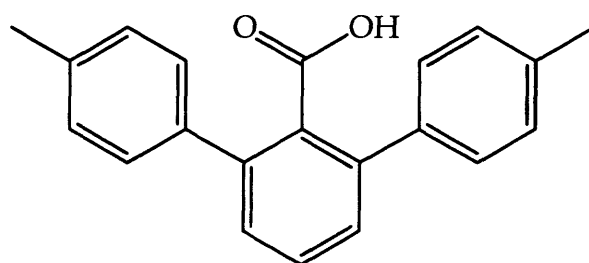


**Figure 1.3.** Schematic representation of an example of a sterically hindered carboxylic acid, 2,6-di(*p*-tolyl)benzoic acid ( $\text{Ar}^{\text{Tol}}\text{CO}_2\text{H}$ ).

## Chapter 2

# A Diiron(II) Diaqua Complex: Modeling Water in the Active Site of sMMOH<sub>red</sub>

## Introduction

Soluble methane monooxygenase catalyzes the hydroxylation of methane to methanol.<sup>1,2</sup> In our group, we would like to replicate this function by using a small molecule complex that models the active sites of the hydroxylase component of sMMO (sMMOH). The reduced form of sMMOH contains two diiron(II) centers, each comprising four carboxylates, two nitrogen donors, and two water molecules (Figure 2.1). Our goal is to synthesize a diferrous complex containing water and then to study its structural and magnetic properties.

Additionally, the weakly ferromagnetic exchange coupling in the diiron(II) center of sMMOH<sup>3,4</sup> is not completely understood. It has been proposed that it may be associated with the  $\mu$ -1,1-oxygen atom bridge supplied by one of the carboxylate ligands.<sup>5</sup> To address this issue, a number of diferrous model complexes have been synthesized and studied. Interestingly, ferromagnetic exchange coupling in diferrous complexes arises in complexes with two single atom bridges, whereas antiferromagnetic properties characterize complexes with a only one single atom bridge.<sup>6</sup> Unfortunately, the bridging groups in the reported complexes include halides and phenoxides, which are not biologically relevant to the bridging unit in the diferrous core in MMOH. It was therefore of interest to study the magnetic properties of a diferrous complex that is similar to those in the active sites of sMMOH<sub>red</sub> and has the necessary bridging groups to mimic the magnetic properties of the enzyme.

## Experimental

**General Procedures.** Pentane, THF and  $\text{CH}_2\text{Cl}_2$  were saturated with argon and purified by passing over a column of activated  $\text{Al}_2\text{O}_3$  under argon.<sup>7</sup> Sodium 2,6-di-(*p*-tolyl)benzoate ( $\text{NaO}_2\text{CAr}^{\text{Tol}}$ )<sup>8-10</sup> and  $[\text{Fe}_2(\mu\text{-O}_2\text{CAr}^{\text{Tol}})_2(\text{O}_2\text{CAr}^{\text{Tol}})_2(\text{THF})_2]$ <sup>11</sup> were prepared according to published procedures. All other reagents were purchased from commercial sources and used as received. Manipulations of air-sensitive iron(II) complexes were performed under nitrogen in an MBraun glovebox. FT-IR spectra were measured on a Thermo-Nicolet 360 Avatar instrument running OMNIC software.

$[\text{Fe}_2(\mu\text{-O}_2\text{CAr}^{\text{Tol}})_2(\mu\text{-OH})_2(\text{O}_2\text{CAr}^{\text{Tol}})_2(\text{THF})_2]$  (1), **Method A.** A portion of  $\text{NaO}_2\text{CAr}^{\text{Tol}}$  (100 mg, 0.309 mmol) and  $\text{Fe}(\text{BF}_4)_2 \cdot 6\text{H}_2\text{O}$  (52 mg, 0.154 mmol) were stirred in a solution of 3 mL of THF and 9 mL of  $\text{CH}_2\text{Cl}_2$  for 3 days. The solution was filtered twice and pentane was diffused into it. After a few more days, colorless block crystals formed (7 mg, ~ 6% yield) and were analyzed by X-ray crystallography.

$[\text{Fe}_2(\mu\text{-O}_2\text{CAr}^{\text{Tol}})_2(\mu\text{-OH})_2(\text{O}_2\text{CAr}^{\text{Tol}})_2(\text{THF})_2]$  (1), **Method B.** A portion of  $[\text{Fe}_2(\mu\text{-O}_2\text{CAr}^{\text{Tol}})_2(\text{O}_2\text{CAr}^{\text{Tol}})_2(\text{THF})_2]$  (80 mg, 0.055 mmol) was allowed to stir in a solution of 2 mL of THF with 17.7  $\mu\text{L}$  (0.99 mmol) of anaerobic water for 30 min. The solution was filtered and pentane was diffused into it. After a few days, colorless block crystals formed (40 mg, ~ 50% yield) and were analyzed by X-ray crystallography. FT-IR (KBr,  $\text{cm}^{-1}$ ) 3555 (m,  $\nu_{\text{O-H}}$ ), 3424 (w, br,  $\nu_{\text{O-H}}$ ), 3051 (w), 3022 (w), 2918 (m), 1588 (s), 1571 (s), 1514 (s), 1454 (s), 1408 (s), 1381 (s), 1306 (w), 1187 (w), 1110 (w), 1071 (w), 1042 (s), 1019 (m), 890 (w), 854 (w), 836 (m), 822 (s), 802 (s), 796 (m), 787 (m), 765 (s), 736 (m), 713 (w), 701

(m), 584 (m), 547 (m), 523 (s), 468 (w). Anal. Calc. for  $C_{92}H_{88}Fe_2O_{12}$ : C, 73.80; H, 5.92. Found: C, 72.98; H, 5.98%.

**X-ray Crystallography.** Crystals were mounted in Paratone N oil on the ends of glass capillaries and frozen into place under a low-temperature nitrogen cold stream. Data were collected on a Bruker SMART APEX CCD X-ray diffractometer running the SMART software package,<sup>12</sup> with Mo  $K\alpha$  radiation ( $\lambda = 0.71073 \text{ \AA}$ ), and integrated using SAINT software.<sup>13</sup> Details of the data collection and reduction protocols are described elsewhere.<sup>14</sup> The structures were solved by direct methods using SHELXS-97 software<sup>15</sup> and refined on  $F^2$  by using the SHELXTL-97 program<sup>16</sup> incorporated in the SHELXTL software package.<sup>17</sup> Empirical absorption corrections were applied with SADABS,<sup>18</sup> part of the SHELXTL program package. All non-hydrogen atoms were refined anisotropically. In general, hydrogen atoms were assigned idealized positions and given thermal parameters equivalent to either 1.5 (methyl hydrogen atoms) or 1.2 (all other hydrogen atoms) times the thermal parameter of the carbon atom to which each was attached. Hydrogen atoms of the coordinated water molecules were identified from difference Fourier maps. Data collection and experimental details are summarized in Table 2.1 and relevant interatomic bond lengths and angles are listed in Table 2.2. The complex **1A** refers to the orthorhombic crystals formed via method A. The complex **1B** refers to the monoclinic crystals formed via either method A or B. The crystal structure is shown in Figure 2.2.

**<sup>57</sup>Fe Mössbauer Spectroscopy.** The Mössbauer spectrum was recorded at 4.2 K in the MIT Department of Chemistry Instrumentation Facility on a MS1 spectrometer



(WEB Research Co.) with a  $^{57}\text{Co}$  source in a Rh matrix at room temperature, and fit to Lorentzian line shapes by using the WMOSS plot and fit program.<sup>19</sup> Isomer shifts were referenced to natural abundance Fe foil at room temperature. The sample was prepared by suspending powdered material ( ~ 20 mg, ~ 0.013 mmol) in Apiezon N grease and placing the mixture in a nylon sample holder. The spectrum is displayed in Figure 2.3, and extracted parameters are provided in Table 2.3.

**SQUID Susceptometry.** Magnetic susceptibility data for powdered solids were measured between 2 or 5 and 200 or 300 K with applied magnetic fields of 0.1 or 0.5, 1, 2.5 and 5 T using a Quantum design MPMS SQUID susceptometer. Each sample was loaded in a gel capsule and suspended in a plastic straw. The susceptibilities of the straw and gel capsule were independently determined over the same temperature ranges and fields for correction of their contribution to the total measured susceptibility. For one sample, eicosane was used to hold the sample in place. A blank with the same amount of eicosane in a gel capsule was used over the same temperature range and fields for this correction. The diamagnetic susceptibility of the sample was calculated from Pascal's constants.<sup>20</sup> The saturation magnetization data were fit using the simplex method to find the spin Hamiltonian parameter set yielding the minimum standard quality of fit parameter,  $\chi^2$ .<sup>6,21,22</sup> The coupling constants and zero-field splitting parameters were calculated using a software package<sup>23</sup> and the exchange Hamiltonian in equation 1.

$$H = -2J\mathbf{S}_1 \cdot \mathbf{S}_2 + \sum_i [D_i(S_{zi}^2 - 2) + E_i(S_{xi}^2 - S_{yi}^2) + \beta \mathbf{S}_i \cdot \mathbf{g}_i \cdot \mathbf{H}], \quad i=1, 2 \quad (1)$$

where  $J$  is the isotropic exchange coupling constant,  $D_i$  and  $E_i$  are the axial and rhombic zero-field splitting parameters, and  $\mathbf{g}_i$  are the  $\mathbf{g}$  tensors of the uncoupled sites ( $i = 1, 2$ ). The standard assumption is made that each  $\mathbf{D}_i$  zero-field splitting tensor has the same axes as its  $\mathbf{g}_i$  tensor. The detailed data handling and fitting processes are described in the literature.<sup>6,21,22,24</sup> All calculated parameters for each of the five runs are given in Table 2.4 and relevant plots are in Figure 2.4. Sample 1 was made from material from method B (11.8 mg, 7.88  $\mu\text{mol}$ ), and run with eicosane (20 mg). Sample 2 was made from a mixture of material from methods A and B, (10.4 mg, 6.95  $\mu\text{mol}$ ). Sample 3 was made from material from method A (49.0 mg, 32.7  $\mu\text{mol}$ ). Sample 4 was made from material from method B (11.6 mg, 7.75  $\mu\text{mol}$ ). Sample 5 was made from the same batch as sample 3 (28.7 mg, 19.2  $\mu\text{mol}$ ).

## Results and Discussion

**Synthesis of  $[\text{Fe}_2(\mu\text{-O}_2\text{CAr}^{\text{Tol}})_2(\mu\text{-OH})_2(\text{O}_2\text{CAr}^{\text{Tol}})_2(\text{THF})_2]$  (1).** This synthesis is reported here and has recently been published.<sup>25</sup> Complex 1 was first prepared fortuitously by method A. Since  $[\text{Fe}_2(\mu\text{-O}_2\text{CAr}^{\text{Tol}})_2(\text{O}_2\text{CAr}^{\text{Tol}})_2(\text{THF})_2]$  may be an intermediate in the reaction, the more rational method B was devised, raising the yield significantly.

**Structural Characterization.** Complex 1 is a diferrous, tetra-bridged complex with an Fe-Fe distance of 3.0430(7) Å in the orthorhombic crystal and 3.0583(11) Å in the monoclinic form (Figure 2.2). These distances compare well with those of other diferrous diaqua-bridged complexes, as described in reference 25. The diiron center

straddles a crystallographic inversion center in both crystal forms. Each of the iron centers have distorted octahedral geometries. Two of the O-atoms are donated by the two  $\mu$ -1,3-carboxylate ligands and two by the bridging water molecules. The coordination spheres are completed by a monodentate carboxylate and a THF molecule on each iron center. The THF molecules are situated with an anti disposition. The non-carboxylate bridging molecules are defined as water due to charge considerations, the location of two hydrogen atoms near each of the oxygen atoms during refinement, and the long Fe–O<sub>bridging</sub> distances of 2.3977(16) Å and 2.3262(15) Å in the orthorhombic crystal and 2.270(2) Å and 2.301(3) Å in the monoclinic one. The IR spectra indicate two O–H stretching modes. The peak at 3555 cm<sup>-1</sup> is of medium intensity and relatively sharp, whereas the peak at 3424 cm<sup>-1</sup> is very weak and broad (Figure 2.5). This second peak probably reflects hydrogen bonding to the dangling oxygen atom of one of the carboxylates (O1–H1···O5). The O1···O5 separations of 2.588(2) Å in the orthorhombic space group and 2.527(3) Å in the monoclinic space group reveal strong H-bonding interactions. Although a few mono-aqua-bridged diiron(II) complexes have been reported,<sup>26-28</sup> this molecule is one of the first diferrous diaqua-bridged complexes in the literature.<sup>25</sup> Diaqua-bridged complexes with carboxylate-rich environments are known for other first row transition metals, such as Co and Ni.<sup>29</sup> The methodologies for the synthesis of these complexes were analogous to those presented here. The dicobalt(II) diaqua complex, [Co<sub>2</sub>( $\mu$ -OH<sub>2</sub>)<sub>2</sub>( $\mu$ -O<sub>2</sub>CAr<sup>Tol</sup>)<sub>2</sub>(O<sub>2</sub>CAr<sup>Tol</sup>)<sub>2</sub>(C<sub>5</sub>H<sub>5</sub>N)<sub>2</sub>], was made by adding water to the preassembled starting dicobalt(II) species. The dinickel(II) diaqua complex, [Ni<sub>2</sub>( $\mu$ -HO···H)( $\mu$ -O<sub>2</sub>CAr<sup>Tol</sup>)<sub>2</sub>(O<sub>2</sub>CAr<sup>Tol</sup>)<sub>2</sub>(C<sub>5</sub>H<sub>5</sub>N)<sub>2</sub>], was made by using a hydrated starting

complex,  $\text{Ni}(\text{NO}_3)_2 \cdot 6\text{H}_2\text{O}$ . Other diaqua dinickel(II) and dicobalt(II) complexes without carboxylate-rich environments are known as well.<sup>30,31</sup> These complexes used similar synthetic methods to those described above.

It is interesting that, when synthesized by different methods, the same complex, **1**, is crystallized in different space groups (Table 2.1). Orthorhombic crystals were not encountered from method B, but both monoclinic and orthorhombic crystals form in method A. There are distinct differences in the two crystal morphologies. Both are colorless, but the monoclinic crystals are rhombohedral blocks whereas the orthorhombic ones resemble dodecahedra. The orthorhombic crystals may not form in method B because only the crystallization conditions of method A favor both forms. Since solvent is never present in the lattice, though, this suggestion cannot be substantiated. The THF molecules are oriented differently in the two crystal forms, as seen in Figure 2.6, which shows views down the Fe-Fe vector. Both forms have two asymmetrically bridged water molecules, and the  $\text{Fe}-\text{O}_{\text{water}}$  distances differ by  $\sim 0.13 \text{ \AA}$  (Table 2.2). These slight structural differences may be a consequence of the different packing arrangements.

**Mössbauer Spectroscopic Properties.** The zero-field Mössbauer spectrum of the powdered sample was recorded at 4.2 K. Only one quadrupole doublet is present, as expected for two iron centers related by a crystallographic inversion center. The isomer shift and quadrupole splitting parameters are consistent with a high-spin diiron(II) complex with N or O coordinated ligands.<sup>32</sup>

**Magnetic Properties.** The exchange coupling constant<sup>33</sup> in  $\text{sMMOH}_{\text{red}}$  from *Methylosinus trichosporium* OB3b is around  $0.3 \text{ cm}^{-1}$ , revealing weak ferromagnetism.<sup>3,4</sup> Complex **1** is also weakly ferromagnetic, with a coupling constant of around  $0.947 \text{ cm}^{-1}$  (Table 2.4). There were some difficulties with reproducibility, however, as described below. The parameters were obtained assuming the two iron sites to be identical. This restriction, as well as those described above, were chosen so as not to over-parameterize the system. Also, the Mössbauer spectrum supports this assumption, since only one quadrupole doublet is present.

There were many problems encountered in reproducing the SQUID magnetic data, as can be seen in Table 2.4, where the coupling constants and zero-field splitting parameters for each of the 5 runs are given. The origin of this disparity is thought to be the presence of the two different morphologies, water loss and/or oxidation.

The different morphologies have different bridging distances and angles, which should in turn affect the coupling parameters. Interestingly, a sample from method A (sample 3) and a sample from method B (sample 4) have very similar coupling constants.

Another reason could be water loss. The Fe–O distances are longer than encountered in other diferrous water complexes,<sup>25-28</sup> suggesting that they are very weakly bound. This suggestion is not supported by spectroscopy, however. An IR spectrum was taken of material that was stored in the glove box for months and it still revealed bound water. Also, a sample was crushed and a portion was used immediately as SQUID sample #3, while another portion was left to sit for three days

before use as sample #5. As a crystal there is a large barrier to the loss of water, but as a powder, this barrier is lower. In addition, sample #5 was also run to only 200 K to see whether bringing the sample to 300 K under vacuum in the instrument was facilitating water loss. The results of the two runs were identical. Considering that there was a trend of weak ferromagnetic coupling (that will be discussed below), this result also suggests that the water molecules remained bound, because a change in the bridging ligands would most likely lead to a more dramatic change in the magnetic properties.

Another possibility is that oxidation caused the irreproducibility. When oxidized the sample is pale yellow. There was no noticeable color change in the sample after the run, however, suggesting that oxidation is not the origin of our problems.

There were some consistencies in the results, however. All of the samples were weakly ferromagnetically coupled with  $J$  values ranging from  $0.892 \text{ cm}^{-1}$  to  $10.595 \text{ cm}^{-1}$ . A small  $J$  value is expected for a complex with only  $\mu$ -1,3-carboxylate and water bridging moieties.<sup>26,34,35</sup> Three of the five samples (3 - 5) matched each other very well and had an average  $J$  value of  $0.947 \text{ cm}^{-1}$ . The other parameters, such as the zero-field splitting parameters and  $g$  values, varied greatly. The basic shape of the  $\mu_{\text{eff}}$  vs.  $T$  curves for these three samples shows an increase in  $\mu_{\text{eff}}$  with decreasing temperature, which is characteristic of ferromagnetic coupling.<sup>6,23</sup> The sudden decrease at around 8 K is due to zero-field splitting (ZFS).<sup>36-38</sup> The two samples taken from the very same batch (3 and 5) do have very similar values for all four parameters, showing some internal consistency. One troubling feature with that data is that the  $g$  value is just under 2.00, 1.987 and 1.960, which is unknown for a high spin diiron(II) complex and more indicative of a

mixed valent species.<sup>38-40</sup> The origin of these variations in the magnetic properties from sample to sample remains unknown.

The diferrous complex **1** has four bridging ligands, two water molecules and two  $\mu$ -1,3-carboxylates. It is unlikely that these carboxylates are the cause of the observed exchange coupling, because a single-atom bridged molecule provides better overlap, and similar complexes without the water bridges are antiferromagnetic.<sup>11,41</sup> Therefore, the coupling must be due to the two water bridges. This finding suggests that in  $s\text{MMO}_{\text{red}}$ , at least one of the water molecules may lead to the slight ferromagnetism of the protein. Since two single atom bridging moieties are usually needed to explain ferromagnetism, the magnetic properties of  $s\text{MMOH}_{\text{red}}$  may be due to the  $\mu$ -1,1-carboxylate bridge and a water molecule.

### Summary and Conclusions

The synthesis of an aqua-containing diferrous complex is quite facile. A ferrous salt with coordinated water may be used as starting material, or a small amount of water may be added to the solvent if a preassembled iron complex is employed. In the synthesis of  $[\text{Fe}_2(\mu\text{-O}_2\text{CAr}^{\text{Tol}})_2(\mu\text{-OH}_2)_2(\text{O}_2\text{CAr}^{\text{Tol}})_2(\text{THF})_2]$ , there are two types of crystals that form, the molecular structures in which are nearly identical, as seen by X-ray crystallography. The Mössbauer data confirm the presence of high spin ferrous atoms with very similar environments and the absence of paramagnetic impurities, at least within the limits of the sensitivity of this technique.

In this small molecule complex, the coupling is due to the presence of two in-plane bridging water molecules. It is probable that the ferromagnetic nature of  $s\text{MMO}_{\text{red}}$  is due to the presence of two single atom bridges, most likely one water molecule and the  $\mu$ -1,1-coordinated carboxylate residue.



**References and Notes**

\* A portion of this work has appeared previously in Yoon, S.; Kelly, A. E.; Lippard, S.J. *Polyhedron* **2004**, in press.

1. Du Bois, J.; Mizoguchi, T. J.; Lippard, S. J. *Coord. Chem. Rev.* **2000**, *200–202*, 443–485.
2. Merckx, M.; Kopp, D. A.; Sazinsky, M. H.; Blazyk, J. L.; Müller, J.; Lippard, S. J. *Angew. Chem. Int. Ed.* **2001**, *40*, 2782–2807.
3. Hendrich, M. P.; Münck, E.; Fox, B. G.; Lipscomb, J. D. *J. Am. Chem. Soc.* **1990**, *112*, 5861–5865.
4. Pulver, S.; Froland, W. A.; Fox, B. G.; Lipscomb, J. D.; Solomon, E. I. *J. Am. Chem. Soc.* **1993**, *115*, 12409–12422.
5. Solomon, E. I.; Brunold, T. C.; Davis, M. I.; Kemsley, J. N.; Lee, S.-K.; Lehnert, N.; Neese, F.; Skulan, A. J.; Yang, Y.-S.; Zhou, J. *Chem. Rev.* **2000**, *100*, 235–349.
6. Hendrich, M. P.; Day, E. P.; Wang, C.-P.; Synder, B. S.; Holm, R. H.; Münck, E. *Inorg. Chem.* **1994**, *33*, 2848–2856.
7. Pangborn, A. B.; Giardello, M. A.; Grubbs, R. H.; Rosen, R. K.; Timmers, F. J. *Organometallics* **1996**, *15*, 1518–1520.
8. Du, C.-J. F.; Hart, H.; Ng, K.-K. *J. Org. Chem.* **1986**, *51*, 3162–3165.
9. Saednya, A.; Hart, H. *Synthesis* **1996**, *12*, 1455–1458.
10. Chen, C.-T.; Siegel, J. S. *J. Am. Chem. Soc.* **1994**, *116*, 5959–5960.
11. Lee, D.; Lippard, S. J. *Inorg. Chem.* **2002**, *41*, 2704–2719.

12. *SMART v5.626: Software for the CCD Detector System*; Bruker AXS: Madison, WI, 2000.
13. *SAINT v5.01: Software for the CCD Detector System*; BRUKER AXS: Madison, WI, 1998.
14. Kuzelka, J., Mukhopadhyay, S.; Spingler, B.; Lippard, S. J. *Inorg. Chem.* **2004**, *43*, 1751–1761.
15. Sheldrick, G. M. *SHELXS-97: Program for the Solution of Crystal Structure*; University of Göttingen: Göttingen, Germany, 1997.
16. Sheldrick, G. M. *SHELXL-97: Program for the Solution of Crystal Structure*; University of Göttingen: Göttingen, Germany, 1997.
17. *SHELXTL v5.10: Program Library for Structure Solution and Molecular Graphics*; BRUKER AXS: Madison, WI, 1998.
18. Sheldrick, G. M. *SADABS: Area-Detector Absorption Correction*; University of Göttingen: Göttingen, Germany, 1997.
19. Kent, T. A. *WMoss v2.5: Mössbauer Spectral Analysis Software*; WEB Research Co.: Minneapolis, MN, 1998.
20. Carlin, R. L. *Magnetochemistry*; Springer-Verlag: New York, 1986.
21. Day, E. P. *Meth. Enzymol.* **1993**, *227*, 437–463.
22. Hendrich, M. P.; Pearce, L. L.; Que, L., Jr.; Chasteen, N. D.; Day, E. P. *J. Am. Chem. Soc.* **1991**, *113*, 3039–3044.
23. Kent, T. A. *WMAG*; WEB Research Co.: Edina, MN.

24. Karlin, K. D.; Nanthakumar, A.; Fox, S.; Murthy, N. N.; Ravi, N.; Huynh, B. H.; Orosz, R. D.; Day, E. P. *J. Am. Chem. Soc.* **1994**, *116*, 4753–4763.
25. Yoon, S.; Kelly, A. E.; Lippard, S. J. *Polyhedron* **2004**, in press.
26. Hagan, K. S.; Lachicotte, R. *J. Am. Chem. Soc.* **1992**, *114*, 8741–8742.
27. Reynolds, R. A., III.; Dunham, W. R.; Coucouvanis, D. *Inorg. Chem.* **1998**, *37*, 1232–1241.
28. Coucouvanis, D.; Reynolds, R. A., III.; Dunham, W. R. *J. Am. Chem. Soc.* **1995**, *117*, 7570–7571.
29. Lee, D.; Hung, P.-L.; Spingler, B.; Lippard, S. J. *Inorg. Chem.* **2002**, *41*, 521–531.
30. Barrios, A. M.; Lippard, S. J. *J. Am. Chem. Soc.* **1999**, *121*, 11751–11757.
31. Hänggi, G.; Schmalle, H.; Dubler, E. *Acta Cryst.* **1992**, *C48*, 1008–1012.
32. Münck, E. In *Physical Methods in Bioinorganic Chemistry: Spectroscopy and Magnetism*; Que, L., Jr., Ed.; University Science Books: Sausalito, CA, 2000, pp 287–319.
33. All exchange coupling constants ( $J$ ) not calculated for this paper are given using  $H = -2JS_1S_2$ .
34. Reem, R. C.; Solomon, E. I. *J. Am. Chem. Soc.* **1984**, *106*, 8323–8325.
35. Reem, R. C.; Solomon, E. I. *J. Am. Chem. Soc.* **1987**, *109*, 1216–1226.
36. Kennedy, B. J.; Murray, K. S. *Inorg. Chem.* **1985**, *24*, 1552–1557.
37. Wiegardt, K.; Bossek, U.; Nuber, B.; Weiss, J.; Bonvoisin, J.; Corbella, M.; Vitols, S. E.; Girerd, J. J. *J. Am. Chem. Soc.* **1988**, *110*, 7398–7411.

38. Girerd, J.-J.; Journaux, Y. In *Physical Methods in Bioinorganic Chemistry: Spectroscopy and Magnetism*; Que, L., Jr., Ed.; University Science Books: Sausalito, CA, 2000, pp 321–374.
39. Davydov, A.; Davydov, R.; Gräslund, A.; Lipscomb, J. D.; Andersson, K. K. *J. Biol. Chem.* **1997**, *272*, 7022–7026.
40. Sands, R. H.; Dunham, W. R. *Q. Rev. Biophys.* **1975**, *7*, 443–504.
41. Goodwin, J. C.; Price, D. J.; Heath, S. L. *Dalton Trans.* **2004**, advanced article.

**Table 2.1.** Summary of X-ray crystallographic information

	<b>1A<sup>a</sup></b>	<b>1B</b>
Formula	C <sub>92</sub> H <sub>88</sub> Fe <sub>2</sub> O <sub>12</sub>	C <sub>92</sub> H <sub>88</sub> Fe <sub>2</sub> O <sub>12</sub>
Fw	1497.32	1497.32
space group	Pbca	P2 <sub>1</sub> /n
<i>a</i> , Å	19.884(4)	13.536(5)
<i>b</i> , Å	18.358(4)	14.234(5)
<i>c</i> , Å	20.773(4)	20.251(7)
α, deg		
β, deg		104.706(7)
γ, deg		
<i>V</i> , Å <sup>3</sup>	7583(3)	3774(2)
<i>Z</i>	4	2
<i>T</i> , °C	-100	-100
ρ <sub>calcd</sub> , g cm <sup>-3</sup>	1.312	1.318
μ(M <sub>o</sub> Kα), mm <sup>-1</sup>	0.447	0.450
θ range, deg	1.80-28.35	1.77-25.50
Total no. of data	65007	28433
no. of unique data	9257	7019
no. of parameters	490	490
R <sup>a</sup>	0.0479	0.0561
wR <sup>2b</sup>	0.1054	0.1087
Max, min peaks, e Å <sup>-3</sup>	0.636, -0.383	0.264, -0.400

$$^a R = \frac{\sum ||F_o| - |F_c||}{\sum |F_o|}, \quad ^b wR^2 = \left\{ \frac{\sum [w(F_o^2 - F_c^2)^2]}{\sum [w(F_o^2)^2]} \right\}^{1/2}.$$

<sup>a</sup> It is important to note that both monoclinic and orthorhombic crystals form via method A.

**Table 2.2.** Selected bond lengths (Å) and angles (deg) for **1A** and **1B**

	<b>1A</b>	<b>1B</b>
Fe1···Fe1A	3.0430(7)	3.0583(11)
Fe1–O1	2.3977(16)	2.270(2)
Fe1A–O1	2.3262(15)	2.301(3)
Fe1–O2	2.0232(13)	2.068(2)
Fe1–O3	2.0322(13)	2.020(2)
Fe1–O4	2.0442(13)	2.053(2)
Fe1–O6	2.1415(15)	2.098(2)
Fe1–O1–Fe1A	80.19(5)	83.98(8)
O1–Fe1–O1A	99.81(5)	96.02(8)
O2–Fe1–O3	157.21(5)	156.77(9)
O1–Fe1–O4	87.78(5)	89.40(9)
O1–Fe1–O6	169.88(6)	177.23(9)
O2–Fe1–O4	105.91(6)	94.70(9)
O3–Fe1–O4	91.26(5)	104.77(9)
O2–Fe1–O6	89.36(5)	96.95(9)
O3–Fe1–O6	106.48(6)	96.33(9)
O4–Fe1–O6	87.89(5)	87.85(9)
O2–Fe1–O1	83.05(5)	83.64(10)
O3–Fe1–O1	82.76(5)	84.02(10)
O2–Fe1–O1A	85.81(6)	78.00(9)
O3–Fe1–O1A	79.16(5)	83.82(10)
O4–Fe1–O1A	166.83(6)	170.32(10)
O6–Fe1–O1A	86.23(5)	86.75(8)
O5···O1	2.588(2)	2.527(3)

Numbers in parentheses are estimated standard deviations of the last significant figures. For atom labels, see Figure 2.2.

**Table 2.3.** Summary of Mössbauer parameters recorded at 4.2 K ( $\text{mm s}^{-1}$ )

$\delta$	$\Delta E_0$	$\Gamma$
1.31(2)	2.86(2)	0.24(2)

Table 2.4. SQUID data

Sample	1	2	3	4	5
$D$ ( $\text{cm}^{-1}$ )	-1.481	6.330	-4.303	1.726	-3.698
$E/D$	0.007	0.063	0.008	0.120	0.004
$g$	2.152	1.648	1.960	2.426	1.987
$J$ ( $\text{cm}^{-1}$ )	6.344	10.595	0.897	1.051	0.892
Amount	0.789	0.897	1.157	0.731	1.119
$R\chi^2$	2.926	33.619	1.627	5.607	2.324
$\mu_{\text{eff}}$ in $\mu_B$ at 1T at 5K	8.350	6.390	8.210	8.366	8.256
max $\mu_{\text{eff}}$ in $\mu_B$ at 1T	9.051 (32.7 K)	7.315 (280 K)	8.539 (8 K)	8.628 (8 K)	8.560 (8 K)
$\mu_{\text{eff}}$ in $\mu_B$ at 1T at 200K	8.794	7.164	7.749	7.829	7.650
Sample 1- Material from method B (11.8 mg), run with eicosane (20 mg).					
Sample 2- Material from methods A and B, (10.4 mg).					
Sample 3- Material from method A (49.0 mg).					
Sample 4- Material from method B (11.6 mg).					
Sample 5- Material from same batch as sample 3 (28.7 mg).					



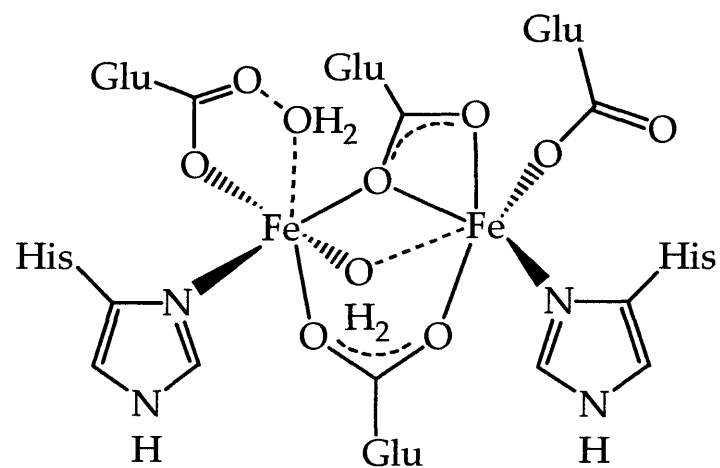


**Figure 2.1.** Detailed representation of the active site of sMMOH<sub>red</sub>.

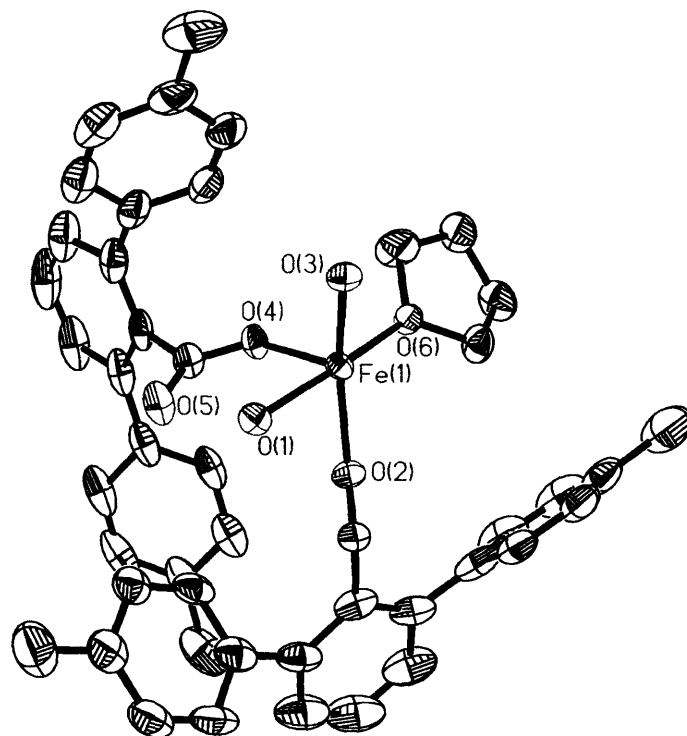
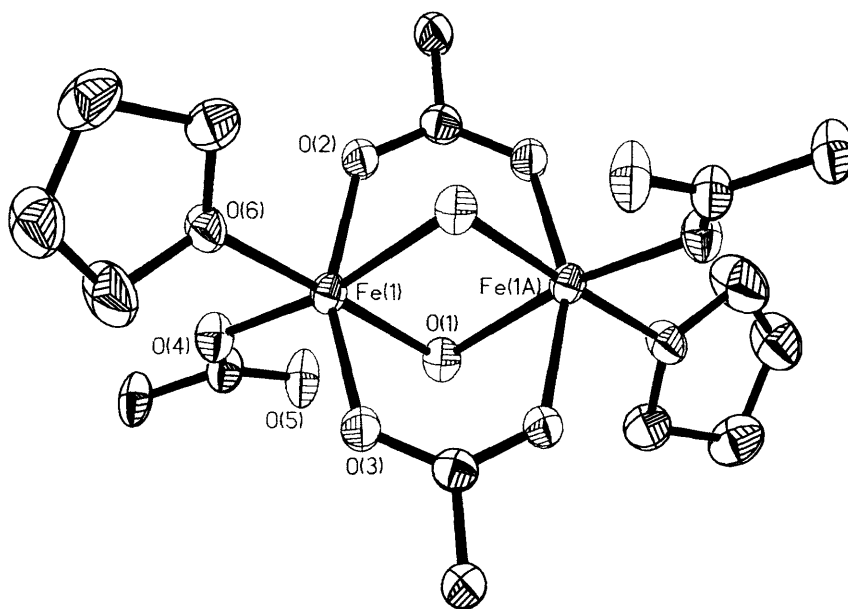


**Figure 2.2.** ORTEP diagrams of 1, both the core and asymmetric unit, showing 50% probability thermal ellipsoids. Hydrogen atoms have been omitted for clarity. These pictures were made using data from a monoclinic crystal.

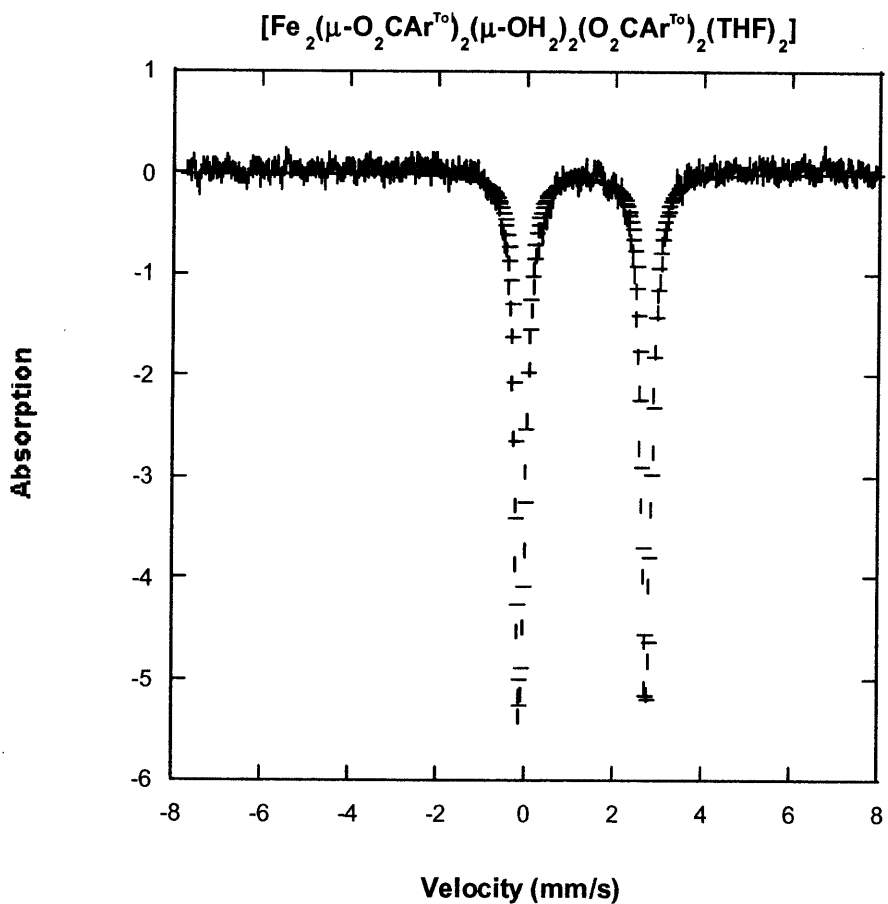


**Figure 2.3.** Zero-field Mössbauer spectrum (experimental data (|), calculated fit (—)) recorded at 4.2 K of a solid sample.

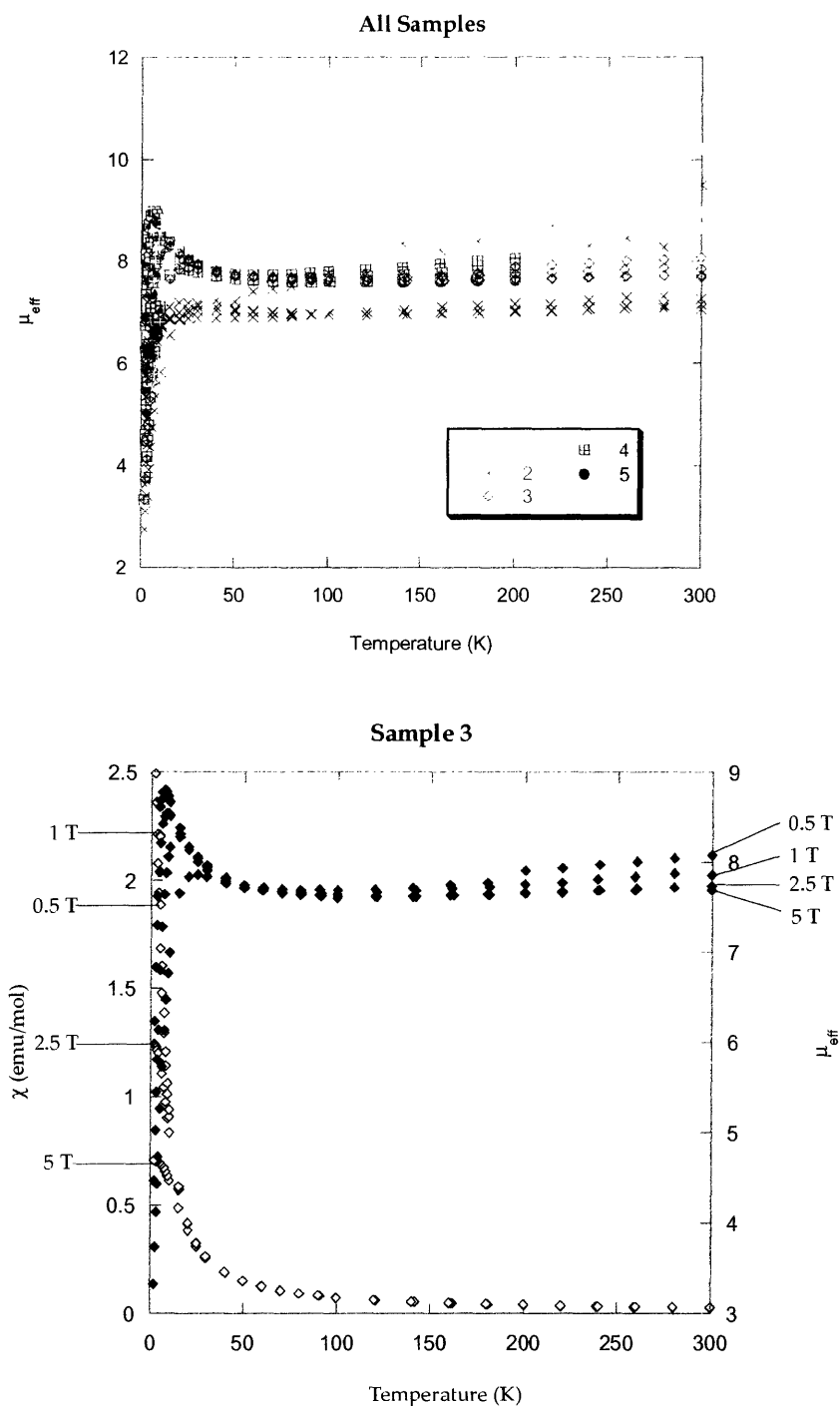


**Figure 2.4.** SQUID spectra. Top: A plot of  $\mu_{\text{eff}}$  vs.  $T$  for all 5 samples run. Bottom: A plot of  $\chi$  vs.  $T$  (open diamonds) and  $\mu_{\text{eff}}$  vs.  $T$  (filled diamonds) for sample 3, a representative sample.

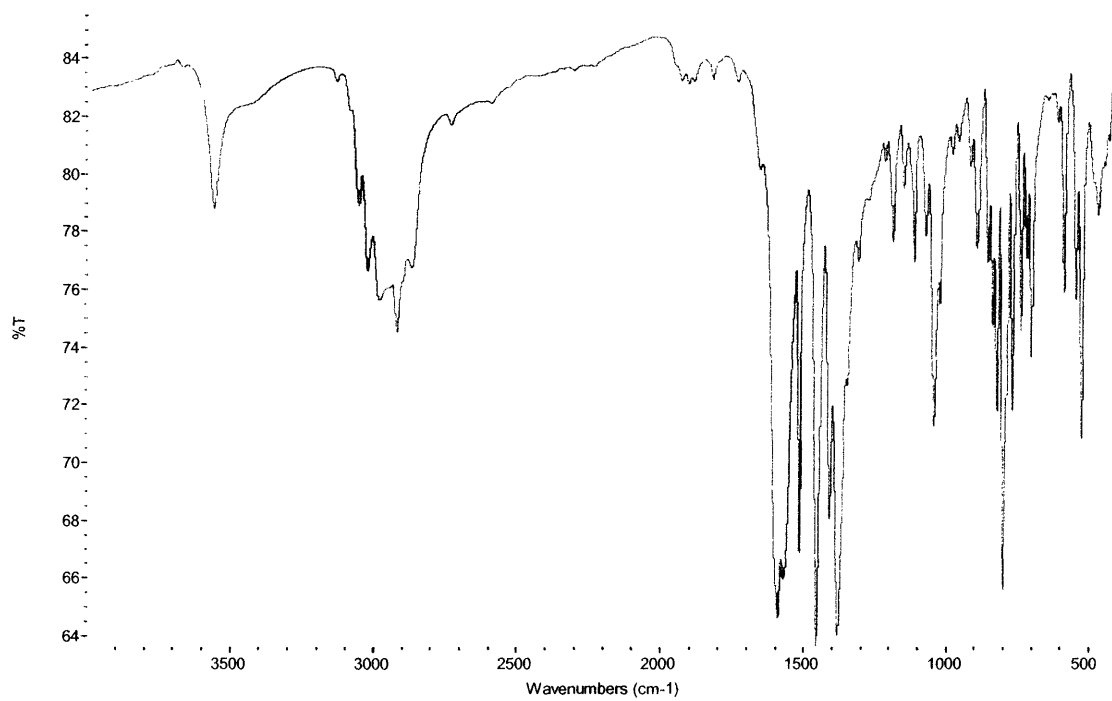


**Figure 2.5.** FT-IR spectrum of  $[\text{Fe}_2(\mu\text{-O}_2\text{CAr}^{\text{Tol}})_2(\mu\text{-OH})_2(\text{O}_2\text{CAr}^{\text{Tol}})_2(\text{THF})_2]$ .

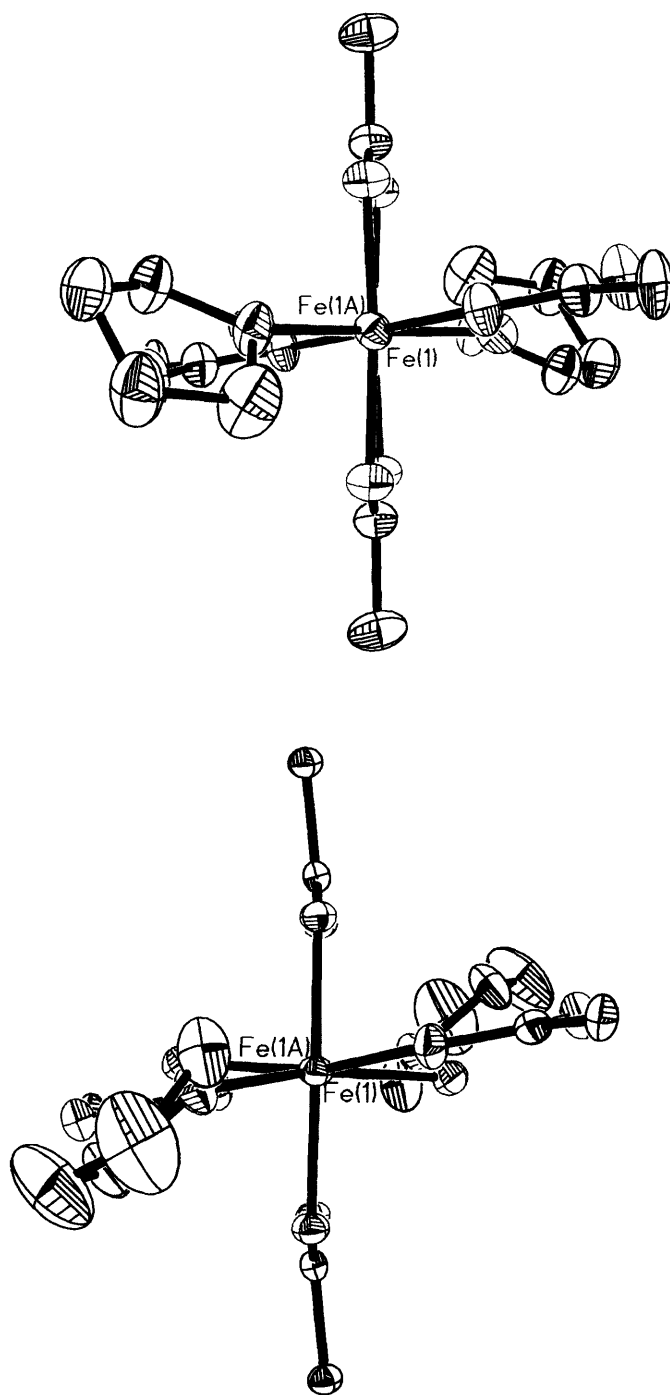


**Figure 2.6.** Figure displaying the difference in THF orientation between the monoclinic (top) and orthorhombic (bottom) crystal structures.

## **Chapter 3**

# **Ligands for Modeling the Syn Disposition of Nitrogen Atoms in the Active Site of MMOH**

## Introduction

The oxidation of methane to methanol in *Methylococcus capsulatus* (Bath) is catalyzed by the enzyme soluble methane monooxygenase (sMMO).<sup>1,2</sup> The active sites of the reduced form of the hydroxylase component, sMMOH<sub>red</sub>, each contain a diiron(II) center with four carboxylates, two nitrogen donors, and two water molecules (Figure 3.1). The reduced form is one of the spectroscopically visible species in the proposed catalytic reaction cycle, an abbreviated version of which is shown in Figure 3.2.

Attempts to model the species involved in the catalytic cycle have taught us much about what types of ligands are useful in preparing a biomimetic diferrous complex. Sterically hindered terphenyl-based carboxylates, such as 2,6-di(*p*-tolyl)benzoate ( $\text{Ar}^{\text{Tol}}\text{CO}_2^-$ ) (Figure 3.3), were used to synthesize complexes of the desired stoichiometry, composed of four carboxylates and two nitrogen donors bound to the diiron center. Unfortunately, when allowed to self-assemble, the nitrogen donors were oriented anti to each other in the product.<sup>3-7</sup> It is necessary for the nitrogen donors to have a syn orientation to model accurately the active sites of sMMOH and perhaps to reproduce the catalytic oxidation of methane.<sup>8</sup>

The most recent attempts at enforcing syn geometry of the nitrogen donors utilized diethynyl benzene as the platform.<sup>9</sup> A series of these compounds were made, of which the diquinoline species, 1,2-bis(3-ethynylquinoline)benzene<sup>10</sup> (BQEB), was the most successful. The steric bulk of the quinoline rings may restrict rotation so that the nitrogen atoms are pointed toward the diiron center (Figure 3.4).



Previously, BQEB was used to synthesize  $[\text{Fe}_2(\mu\text{-OH})(\mu\text{-O}_2\text{CAr}^{\text{Tol}})(\mu\text{-BQEB})(\text{O}_2\text{CAr}^{\text{Tol}})_2(\text{THF})(\text{H}_2\text{O})]$ . Unfortunately, the results were difficult to reproduce. A new ligand framework was therefore designed, using a diethynylbenzene platform with quinoline moieties plus a carboxylate unit installed on the 8-position of each quinoline. With this addition, the N-donor ligand became tetradentate, rather than being able to bind to the metal site only at the two nitrogen atoms. An example of one of these ligands is 1,2-bis(3-ethynyl-8-carboxylatoquinoline)benzene ( $\text{H}_2\text{BCQEB}$ ) (Figure 3.5).<sup>9</sup> The sodium salt of this molecule reacted with  $[\text{Fe}_2(\mu\text{-O}_2\text{CAr}^{\text{Tol}})_2(\text{O}_2\text{CAr}^{\text{Tol}})_2(\text{THF})_2]$ , but crystallization attempts produced only insoluble material. It was postulated that the non-coordinating oxygen atoms of the carboxylate units might bridge to other metal ions in solution, creating insoluble polymers.<sup>9</sup> Using an ester moiety instead of a carboxylate protects these oxygen atoms, allowing for a discrete diferrous complex to be crystallized. When the ethyl ester was used and ethyl groups were added to the benzene backbone (meta to the ethynyl groups) to enhance solubility, the complex  $[\text{Fe}_2(\text{Et}_2\text{BCQEB}^{\text{Et}})(\mu\text{-O}_2\text{CAr}^{\text{Tol}})_3](\text{OTf})$  was isolated, where  $\text{Et}_2\text{BCQEB}^{\text{Et}}$  is 1,2-bis(3-ethynyl-8-carboxylatoquinoline)-4,5-diethylbenzene ethyl ester.<sup>9</sup> This structure has syn nitrogen atoms, as in the active site of  $\text{sMMOH}_{\text{red}}$ . However, a few features are lacking, since this complex has only three carboxylate ligands bound to the diiron unit, rather than the four in the enzyme, creating an undesired positive charge on the complex.

As a second generation approach, bulky alkyl groups were designed to be near the non-coordinated oxygen atoms of  $\text{H}_2\text{BCQEB}$ , in order to block them from binding to any other iron centers without altering the electronic properties of the ligand.

Introduction of isopropyl groups on the 7-position of the quinoline ring would afford the desired species, as depicted in Figure 3.6.

Another approach to the synthesis of a syn-binding N-donor ligand framework is to change the nature of the diethynyl benzene unit. Such a platform would need to be able to compensate for motion around the iron sites during oxygenation, enforce a syn conformation of the nitrogen donors, and facilitate the crystallization of diiron products. Flexibility is important since the active site of sMMOH goes through varied conformations in its reaction cycle (Figure 3.2). For example, the Fe...Fe distance diminishes from 3.3 Å in  $\text{MMOH}_{\text{red}}$ <sup>11,12</sup> to ~ 2.5 Å in the proposed high valent  $\text{Fe}_2^{\text{IV}}(\text{O})_2$  intermediate Q.<sup>13</sup> Since the diethynylbenzene moiety is planar, it may be difficult to crystallize its iron complexes. A platform was desired that was not planar, which would allow for more efficient unit cell packing. Silane moieties were therefore investigated as a replacement for the benzene unit.

Great strides in model chemistry have been made since the introduction of bulky carboxylates. However, it does not appear as if a balance between the steric bulk of the carboxylate and nitrogen donor ligands has yet been found. It seems that small N-donors employed with small carboxylates have the propensity to yield polynuclear compounds,<sup>14,15</sup> which is why carboxylates such as  $\text{Ar}^{\text{Tol}}\text{CO}_2^-$  were introduced. There are many examples of reactions with small nitrogen donors and large carboxylates which yield an anti disposition of N-donors.<sup>3-7</sup> In our research thus far, large nitrogen donors and large carboxylates create materials that are sometimes difficult to crystallize, possibly because they might be oligomeric.<sup>9</sup> Few reactions have been carried out with

large nitrogen donors and smaller carboxylates, however. The *m*-terphenyl carboxylates were very useful when ligands like pyridine were used. However, with such big moieties as BQEB, which have been designed to enforce the syn geometry of the nitrogens, smaller carboxylates may prove to be more suitable. Although BCQEB is large, its design avoids this problem by incorporating two small carboxylate units into the syn N-donor ligand. A large, simple syn nitrogen donating ligand has been designed, 4,6-dibenzofuranbis(isoquinoline), where smaller carboxylates may prove useful in isolating a diiron complex.

## Experimental

**General Procedures.** THF was saturated with argon and purified by passing over a column of activated  $\text{Al}_2\text{O}_3$  under argon.<sup>16</sup> The compounds  $[\text{Fe}_2(\mu\text{-O}_2\text{CAr}^{\text{Tot}})_2(\text{O}_2\text{CAr}^{\text{Tot}})_2(\text{THF})_2]$ <sup>7</sup> and 4,6-dibenzofuranylboronic acid<sup>17</sup> were prepared according to published literature procedures. 1-Bromo-4-isopropyl-2-nitrobenzene was synthesized according to literature with some modification.<sup>18</sup> Instead of distilling the product, purification was performed by precipitating the impurities with hexanes, filtering, and using silica gel column chromatography with 1:20 ethyl acetate/ hexanes. All other reagents were purchased from commercial sources and used as received. All metallation attempts were performed under a nitrogen atmosphere in an MBraun glovebox.

**3-Isopropylphenylamine (1a).** A portion of 1-bromo-4-isopropyl-2-nitrobenzene (100 mg, 0.41 mmol) was dissolved in MeOH (~ 20 mL). A portion of Raney nickel

(assumed to be ~ 10 mol %) was rinsed with MeOH and added to the solution. A hydrogen balloon was attached and the solution was allowed to stir under a hydrogen atmosphere overnight. The solution was filtered and the solvent was removed by rotary evaporation. A portion of NaHCO<sub>3</sub>(aq) (20 mL) was added and the product was extracted with Et<sub>2</sub>O, washed with water, dried over MgSO<sub>4</sub> and filtered. After the solvent was removed by rotary evaporation, the crude product was purified by silica gel column chromatography (1:2 ethyl acetate/ hexanes) to afford the final product (5.5 mg, 10% yield). <sup>1</sup>H NMR (CDCl<sub>3</sub>) δ 1.24 (d, 6H), 2.82 (sept, 1H), 3.62 (bs, 2H), 6.51-6.55 (dd, 1H), 6.58-6.59 (m, 1H), 6.64-6.80 (m, 1H), 7.10 (t, 1H). EI (m/z): Calcd for C<sub>9</sub>H<sub>13</sub>N M<sup>+</sup>, 135; Found 135.

**N-(3-Isopropylphenyl)-2,2-dimethylpropionamide (1b).** The mixed amine products of **1a** (366 mg), some 3-isopropylphenylamine and some halogenated impurities, were stirred in CH<sub>2</sub>Cl<sub>2</sub> (~ 7 mL) at 0 °C. A portion of trimethylacetyl chloride (0.415 mL) was added and then NEt<sub>3</sub> (0.72 mL) was added to the solution, which was stirred at 0 °C for 1 h, then at room temperature for 15 min. After being poured onto ice, the organic layer was separated and the remaining product in the aqueous layer was extracted with ethyl acetate. The solution was washed with brine, dried over MgSO<sub>4</sub> and filtered. After solvent was removed by rotary evaporation, the crude product was purified by silica gel column chromatography (1:1 ethyl acetate/ hexanes), affording the product (279 mg). A percent yield cannot be given, because this material still had some slight impurities that were seen in the <sup>1</sup>H NMR spectrum. <sup>1</sup>H NMR (CDCl<sub>3</sub>) δ 1.25-1.27 (d, 6H), 1.28 (s, 9H), 2.90 (sept, 1H), 6.97-7.00 (m, 1H), 7.25 (t,

1H), 7.30-7.34 (m, 1H), 7.46-7.47 (t, 1H). EI (m/z): Calcd for  $C_{14}H_{21}NO M^+$ , 219; Found 219.

**2-*tert*-Butoxycarbonylamino-6-chlorobenzoic Acid (2a).** A portion of di-*tert*-butyl dicarbonate (669  $\mu$ L, 2.9 mmol) was added to a solution of 2-amino-6-chlorobenzoic acid (500 mg, 2.9 mmol) in THF (20 mL) and allowed to stir for 2 h. Solvent was removed by rotary evaporation, ethyl acetate (15 mL) was added, and the solution was washed 3 $\times$  with brine. The solution was dried over  $Na_2SO_4$ , filtered, and the solvent was removed by rotary evaporation to afford the product (775 mg, 98% yield).  $^1H$  NMR ( $CDCl_3$ )  $\delta$  1.54 (s, 9H), 6.60-6.63 (dd, 1H), 6.77-6.80 (dd, 1H), 7.13 (t, 1H).

**2-*tert*-Butoxycarbonylamino-6-chlorobenzoic Acid Methyl Ester (2b).** To a solution of 2-*tert*-butoxycarbonylamino-6-chlorobenzoic acid (75 mg, 0.276 mmol) in DMF (200  $\mu$ L) was added  $Cs_2CO_3$  (171 mg, 0.525 mmol). The solution was cooled to 0  $^\circ C$  and MeI (17.2  $\mu$ L, 0.276 mmol) was slowly added. The solution was allowed to stir for  $\sim$  1.5 h. Then MTBE/ $H_2O$  (2 mL, 1:1) was added. The organic layer was washed with 10%  $NaHCO_3$ , brine and water. The solution was dried over  $MgSO_4$  and filtered. After the solvent was removed by rotary evaporation, the crude product was purified by silica gel column chromatography (1:5 ethyl acetate/ hexanes) to isolate the product (19 mg,  $\sim$  10% yield).  $^1H$  NMR ( $CDCl_3$ )  $\delta$  1.51 (s, 9H), 3.98 (s, 3H), 7.07-7.10 (dd, 1H), 7.31 (t, 1H), 8.08-8.11 (d+bs, 1H+NH). EI (m/z): Calcd for  $C_{13}H_{16}NO_4Cl M^+$ , 286; Found 285.

**Bis(3-pyridylethynyl)di-*tert*-butylsilane (3a).** A portion of  $^nBuLi$  (3.03 mL (1.6 M in hexanes), 4.85 mmol) was added to a solution of 3-ethynylpyridine (0.5 g, 4.85 mmol) in THF ( $\sim$  50 mL) under nitrogen. The solution was allowed to stir for 3 h. Another

flask was charged with THF (~ 100 mL) and a portion of di-*tert*-butyldichlorosilane (0.512 mL, 2.42 mmol) was added. The contents of this flask were introduced to the first via cannula. The reaction mixture was stirred at 40 °C overnight. The solvent was removed by rotary evaporation and the product was extracted with CH<sub>2</sub>Cl<sub>2</sub>, washed with base (pH ~ 8), dried over MgSO<sub>4</sub> and filtered, yielding clear golden oil. It was further purified by HPLC and dried at 60 °C under reduced pressure to afford a yellow solid (127 mg, 15% yield). Silanes **3b** - **3d** were synthesized in the same manor, but they were not as well characterized. FT-IR (KBr, cm<sup>-1</sup>) 2964 (s) 2933 (s), 2893 (s), 2860 (s), 2163 (s,  $\nu_{\text{C}\equiv\text{C}}$ ), 1470 (s), 1407 (m), 1186 (s), 840 (s), 822 (s), 806 (s). <sup>1</sup>H NMR (CDCl<sub>3</sub>)  $\delta$  1.22 (s, 18H), 7.21-7.25 (m, 2H), 7.72-7.79 (m, 2H), 8.51-8.53 (m, 2H), 8.68-8.71 (m, 2H). ESI-MS (+m/z): Calcd for C<sub>22</sub>H<sub>27</sub>N<sub>2</sub>Si (M+H)<sup>+</sup>, 347.5; Found 347.4.

**4,6-Dibenzofuranbis(isoquinoline) (4)**. A solution of 4,6-dibenzofuranyl-bisboronic acid (500 mg, 1.95 mmol), 4-bromoisoquinoline (813 mg, 3.91 mmol), benzene (20 mL), 2 M Na<sub>2</sub>CO<sub>3</sub>(aq) (10 mL) and EtOH (15 mL) was sparged with Ar for 1 h. A portion of Pd(Ph<sub>3</sub>P)<sub>4</sub> (226 mg, 10 mol %) was added and the solution was sparged again for 30 min before it was heated to reflux overnight. After cooling to room temperature, the solution was poured into ethyl acetate (30 mL) and NaHCO<sub>3</sub> (30 mL). The organic layer was separated and washed with NaHCO<sub>3</sub>, water, and NaHCO<sub>3</sub> again. The solution was dried over MgSO<sub>4</sub>, filtered, and the solvent was removed by rotary evaporation. The crude product was purified by silica gel column chromatography (5:1 ethyl acetate/ hexanes), taken up in CH<sub>2</sub>Cl<sub>2</sub>, and then the solvent was removed by rotary evaporation to yield a white/pale green solid (64.6 mg, 13% yield). FT-IR (NaCl

disk,  $\text{cm}^{-1}$ ) 3055 (w), 2213 (w), 1620 (m), 1569 (m), 1504 (m), 1486 (m), 1427 (s), 1390 (s), 1185 (s), 907 (s), 870 (m), 835 (m), 785 (s), 746 (s), 731 (s).  $^1\text{H}$  NMR ( $\text{CDCl}_3$ )  $\delta$  7.50-7.60 (m, 8H), 7.65-7.68 (m, 2H), 7.91-7.94 (m, 2H), 8.14-8.19 (m, 2H), 8.51 (s, 2H), 9.15 (s, 2H).  $^{13}\text{C}$  NMR ( $\text{CDCl}_3$ , 500 MHz)  $\delta$  154.31, 152.46, 143.4, 134.47, 130.79, 129.78, 128.43, 128.10, 128.03, 127.47, 125.04, 124.96, 123.55, 121.65, 121.06. ESI-MS (+m/z): Calcd for  $\text{C}_{30}\text{H}_{19}\text{N}_2\text{O}$  ( $\text{M}+\text{H}$ ) $^+$ , 423.5; Found 423.4.

**Physical Measurements.** The identities and purities of most of the organic products were verified by  $^1\text{H}$  NMR (300 MHz) and mass spectrometry, either EI or ESI.  $^1\text{H}$  NMR spectra were obtained on a 300 MHz Varian Unity or Mercury spectrometer, and  $^{13}\text{C}$  NMR spectra were recorded on a 500 MHz Varian spectrometer. FT-IR spectra were measured on a Thermo-Nicolet 360 Avatar instrument running OMNIC software.

## Results and Discussion

**Attempts at Incorporating Isopropyl Groups in the BCQEB Design.** The challenge was to incorporate a bulky alkyl group next to each of the non-coordinating oxygen atoms of  $\text{H}_2\text{BCQEB}$ , without altering the electronic properties of the ligand. Introduction of isopropyl groups in the 7-position of the quinoline units is a first effort. Most attempts thus far have been centered on trying to synthesize 2-amino-6-isopropylbenzoic acid (Scheme 3.1). Once this compound is made, the synthesis of the final product  $\text{BICQEB}^{\text{K}}$  can be achieved by using previously planned procedures (Scheme 3.2).<sup>9,19-21</sup> In the successful synthesis of BCQEB, 2-aminobenzoic acid was the starting material. The analogue for BICQEB is 2-amino-6-isopropylbenzoic acid. In the

assembly of the final desired ligand (BICQEB), the added isopropyl group may cause problems not encountered with the less bulky benzoic acid, but such is highly unlikely. When allowed to react with 2 equiv of  $\text{Fe}(\text{OTf})_2 \cdot 2\text{MeCN}$  and  $\text{NaO}_2\text{CAr}^{\text{Tol}}$ , the BICQEB ligand should produce an interesting complex that will help us analyze the effects on the reactivity of the final diiron(II) complexes formed from this line of ligands.

A synthesis was devised to prepare 2-amino-6-isopropylbenzoic acid (Scheme 3.1). First, a pivaloyl residue was used as the protecting group, but the deprotection proved to be difficult. Therefore, the use of a BOC group was later employed, as shown in Scheme 3.1. Unfortunately, the synthesis did not proceed as far in the scheme with the BOC group, because of complications in the reduction of the bromine atom when trying to make 3-isopropylphenylamine. A new route was therefore devised using 2-amino-6-chlorobenzoic acid. Once most of the acidic protons were removed, by using a BOC group and by making the methyl ester, a reaction with  $\text{Fe}(\text{acac})_3$  and isopropylmagnesium chloride was attempted. The GC-MS of the products did not indicate the presence of the desired compound, 2-*tert*-butoxycarbonylamino-6-isopropyl-benzoic acid methyl ester.

**Synthesis of 3-Isopropylphenylamine (1a).** This procedure was adapted from a published literature scheme for the *tert*-butyl analogue.<sup>22</sup> No details were given and the reaction seems to proceed best on a small scale. Pressurizing the hydrogenation reaction, adding excess Ni, and adding Zn with acetic acid after the hydrogenation reaction to help dehalogenate the product, did not result in a significant increase in yield. Fortunately, the product was nearly pure and could be used successfully in



further reactions. The synthesis of this molecule has been published, but none of those routes gave only this isomer in a facile manner.<sup>23-26</sup>

**Synthesis of N-(3-Isopropylphenyl)-2,2-dimethylpropionamide (1b).** This synthesis was adapted from a published literature procedure for a similar compound.<sup>27</sup> The amine can be protected with a BOC group,<sup>28</sup> which should be used in future syntheses due to the ease of its removal.<sup>29,30</sup> Such was not found to be the case for the pivaloyl group. The next step in the synthesis was attempted, making 2-(2,2-dimethylpropionylamino)-6-isopropylbenzoic acid methyl ester (1c), and the proper mass was identified (EI (m/z): Calcd for C<sub>16</sub>H<sub>23</sub>NO<sub>3</sub> M<sup>+</sup>, 277.4; Found 277). However, it was too impure for the <sup>1</sup>H NMR to be assigned so the identity of this product is not known. A deprotection of this material was attempted, but the final product was never isolated.

**Synthesis of 2-tert-Butoxycarbonylamino-6-chlorobenzoic Acid (2a) and 2-tert-Butoxycarbonylamino-6-chlorobenzoic Acid Methyl Ester (2b).** These syntheses were adapted from literature<sup>29,31</sup> in hopes of using iron coupling chemistry to form the desired 2-amino-6-isopropylbenzoic acid.<sup>32</sup>

**Design and Synthesis of Silanes (3a - 3d).** Models of sMMOH<sub>red</sub> have been synthesized utilizing a diethynylbenzene backbone to obtain the desired syn geometry of the nitrogen donors.<sup>9</sup> The success of this moiety may be its ability to allow for motion in the diferrous core while still enforcing a syn conformation of the nitrogen donors. Unfortunately, it is also planar which may make it difficult to crystallize. Silanes were chosen since they would not be planar and may permit changes in the Fe...Fe distance. The syntheses of the silanes bis(3-pyridylethynyl)di-tert-butylsilane

(3a), bis(3-pyridylethynyl)diphenylsilane (3b), bis(3-quinolyethynyl)di-*tert*-butylsilane (3c), and bis(3-quinolyethynyl)diphenylsilane (3d) were attempted (Figure 3.7). They were adapted from the syntheses of similar silanes in literature.<sup>33-35</sup> The products were isolated in low yield and characterized by <sup>1</sup>H NMR and mass spectrometry. Unfortunately, difficulties in purification and decomposition of the final products, due to air or light (most likely water vapor in the air), led us to abandon this approach. Also, attempts at metallation never resulted in the formation of crystals. Recent silicon chemistry, mainly the syntheses of 1,3-bis(2-pyridylethynyl)-1,1,3,3-tetramethyldisiloxane and 1,2-bis(2-pyridyl-ethynyl)-1,1,2,2-tetramethyldisilane, have given reason possibly to revisit this project.<sup>36</sup>

**Synthesis of 4,6-Dibenzofuranbis(isoquinoline) (4) and Attempts at Metallation.** The desired ligand was prepared in two steps (Scheme 3.3) using a synthesis adapted from literature.<sup>17</sup> This final ligand has been allowed to react with Fe(OTf)<sub>2</sub>·2 MeCN and the sodium salts of either trifluoroacetate, acetate, benzoate, anthracene-9-carboxylate, or the Ar<sup>4F-Ph</sup>CO<sub>2</sub><sup>-</sup> carboxylate, in addition to the Ar<sup>Tol</sup>CO<sub>2</sub><sup>-</sup> carboxylate. The reactions instantly turned from white to yellow or pale yellow to orange. Crystallizations were impossible on the small scale used (25 mg of the N-donor ligand). The reaction mixtures did not become homogeneous in the organic solvents used (THF, CH<sub>2</sub>Cl<sub>2</sub>, and THF with MeCN and CH<sub>2</sub>Cl<sub>2</sub>) and never gave X-ray quality crystals.

## Conclusions and Implications for Future Work

One of the goals of our project was to create a nonplanar substitute for the diethynylbenzene backbone, which can also accommodate varying Fe...Fe distances. The design of the silane unit seemed promising but the low yield and propensity for decomposition led us to abandon this approach.

The most important goal was to add a sterically hindered group to BCQEB such as an isopropyl group to prevent the non-chelating oxygen from binding to other molecules or metal ions. A recently developed route started with 2-amino-6-chlorobenzoic acid. Once most of the acidic protons were removed by using a BOC group and by making the methyl ester, a reaction with  $\text{Fe}(\text{acac})_3$  and isopropylmagnesium chloride was attempted unsuccessfully. If a triflate rather than the chloro group is used, the substitution is supposed to be facile.<sup>32</sup> Instead, it seems more desirable to make the quinoline first and then do the substitution reaction. A new route (Scheme 3.4) was devised, which reduces the number of steps drastically, compared to the route outlined in Scheme 3.1. This approach should increase the yield and allow for implementation of the chemistry depicted in Scheme 3.2 for eventual isolation of the final product. Once BICQEB has been isolated, it will be allowed to react with  $\text{Fe}(\text{OTf})_2 \cdot 2 \text{ MeCN}$  and  $\text{NaO}_2\text{CAr}^{\text{Tol}}$  in an effort to synthesize a diiron(II) product. The ideal product, shown in Figure 3.6, would be a diferrous complex with syn nitrogen donors and four carboxylate ligands. Then it could be allowed to react with dioxygen in order to analyze possible intermediate(s) formed and to probe the reactivity.

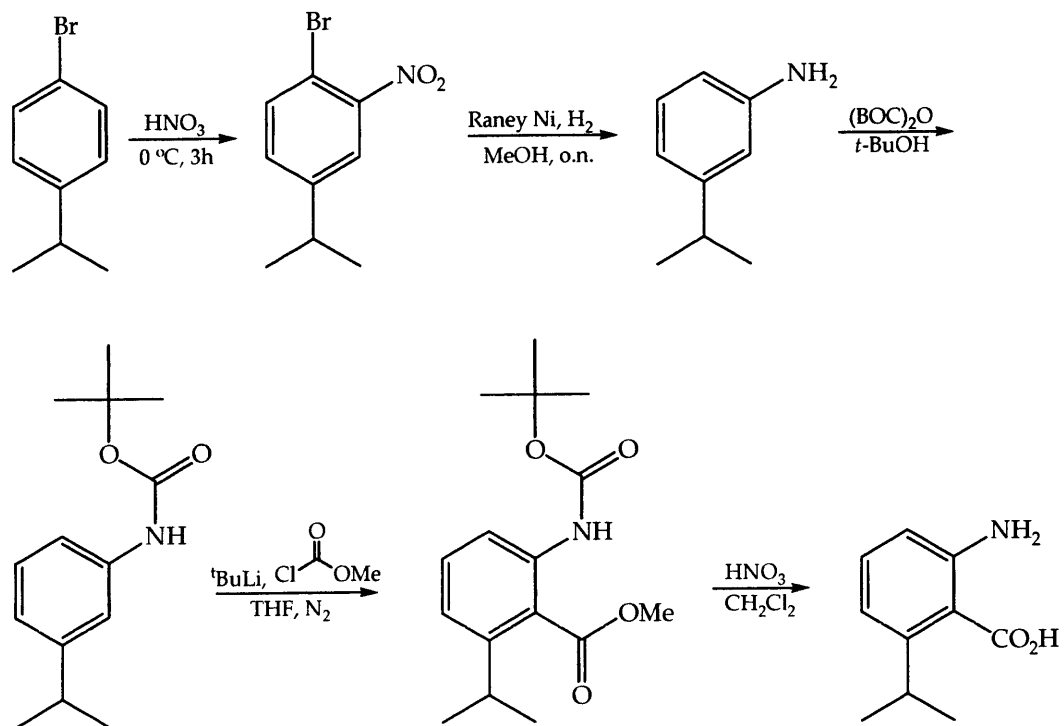
Other future goals include the syntheses of new diiron(II) complexes to address the issue of balance in steric hindrance between the carboxylate and N-donor ligands. It has been proposed that the success of  $\text{Na}_2\text{BCQEB}^{\text{Et}}$  is due to the balance between the sterically encumbered  $\text{Ar}^{\text{tol}}\text{CO}_2^-$  carboxylates and the smaller carboxylate units of the N-donor ligand. Therefore, work with the 4,6-dibenzofuranbis(isoquinoline) ligand should be continued in order to find the right balance of size of nitrogen donors and carboxylate ligands, especially when larger nitrogen donors must be employed to achieve the proper disposition of nitrogen atoms at the diiron center.

**References**

1. Du Bois, J.; Mizoguchi, T. J.; Lippard, S. J. *Coord. Chem. Rev.* **2000**, *200–202*, 443–485.
2. Merckx, M.; Kopp, D. A.; Sazinsky, M. H.; Blazyk, J. L.; Müller, J.; Lippard, S. J. *Angew. Chem. Int. Ed.* **2001**, *40*, 2782–2807.
3. Lee, D.; Lippard, S. J. *J. Am. Chem. Soc.* **2001**, *123*, 4611–4612.
4. Lee, D.; Hung, P.-L.; Spingler, B.; Lippard, S. J. *Inorg. Chem.* **2002**, *41*, 521–531.
5. Lee, D.; Lippard, S. J. *Inorg. Chem.* **2002**, *41*, 827–837.
6. Lee, D.; Pierce, B.; Krebs, C.; Hendrich, M. P.; Huynh, B. H.; Lippard, S. J. *J. Am. Chem. Soc.* **2002**, *124*, 3993–4007.
7. Lee, D.; Lippard, S. J. *Inorg. Chem.* **2002**, *41*, 2704–2719.
8. Baik, M.-H.; Lippard, S. J. Unpublished results.
9. Kuzelka, J.; Farrell, J. R.; Lippard, S. J. *Inorg. Chem.* **2003**, *42*, 8652–8662.
10. Rawat, D. S.; Benites, P. J.; Incarvito, C. D.; Rheingold, A. L.; Zaleski, J. M. *Inorg. Chem.* **2001**, *40*, 1846–1857.
11. Whittington, D. A.; Lippard, S. J. *J. Am. Chem. Soc.* **2001**, *123*, 827–838.
12. LeCloux, D. D.; Barrios, A. M.; Mizoguchi, T. J.; Lippard, S. J. *J. Am. Chem. Soc.* **1998**, *120*, 9001–9014.
13. Tolman, W. B.; Que, L., Jr. *J. Chem. Soc., Dalton Trans.* **2002**, *5*, 653–660.
14. Goldberg, D. P.; Telser, J.; Bastos, C. M.; Lippard, S. J. *Inorg. Chem.* **1995**, *34*, 3011–3024.

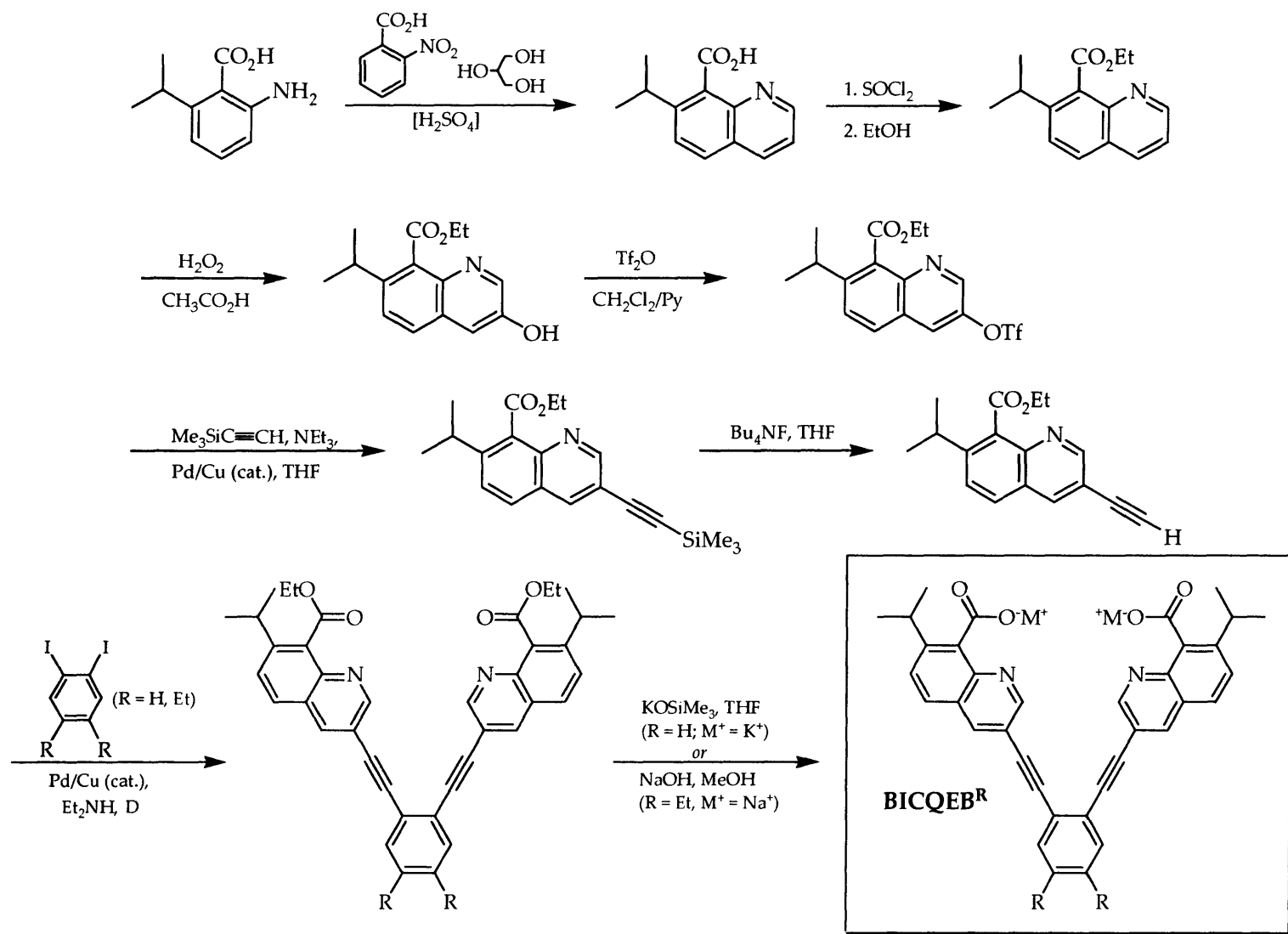
15. Boudalis, A. K.; Lalioti, N.; Spyroulias, G. A.; Raptopoulou, C. P.; Terzis, A.; Tangoulis, V.; Perlepes, S. P. *J. Chem. Soc., Dalton Trans.* **2001**, 7, 955–957.
  16. Pangborn, A. B.; Giardello, M. A.; Grubbs, R. H.; Rosen, R. K.; Timmers, F. J. *Organometallics* **1996**, 15, 1518–1520.
  17. Schwartz, E. B.; Knobler, C. B.; Cram, D. J. *J. Am. Chem. Soc.* **1992**, 114, 10775–10784.
  18. Hays, S. J.; Caprathe, B. W.; Gilmore, J. L.; Amin, N.; Emmerling, M. R.; Michael, W.; Nadimpalli, R.; Nath, R.; Raser, K. J.; Stafford, D.; Watson, D.; Wang, K.; Jaen, J. C. *J. Med. Chem.* **1998**, 41, 1060–1067.
  19. Campbell, K. N.; Kerwin, J. F.; LaForge, R. A.; Campbell, B. K. *J. Am. Chem. Soc.* **1946**, 68, 1844–1846.
  20. Ochiai, E.; Kaneko, C.; Shimada, I.; Murata, Y.; Kosuge, T.; Miyashita, S.; Kawasaki, C. *Chem. Pharm. Bull.* **1960**, 8, 126–130.
  21. Zhou, Q.; Carroll, P. J.; Swager, T. M. *J. Org. Chem.* **1994**, 59, 1294–1301.
  22. Prasad, J. V. N. V.; Panapoulous, A.; Rubin, J. R. *Tetrahedron Lett.* **2000**, 41, 4065–4068.
  23. Attinà, M.; Cacace, F.; de Petris, G. *J. Am. Chem. Soc.* **1985**, 107, 1556–1561.
  24. Gilman, H.; Avakian, S.; Benkeser, R. A.; Broadbent, H. S.; Clark, R. M.; Karmas, G.; Marshall, F. J.; Masie, S. M.; Shirley, D. A.; Woods, L. A. *J. Org. Chem.* **1954**, 19, 1067–1079.
  25. Attinà, M.; Cacace, F. *J. Am. Chem. Soc.* **1983**, 105, 1122–1126.
-

26. Takeuchi, H.; Adachi, T.; Nishiguchi, H.; Itou, K.; Koyama, K. *J. Chem. Soc. Perkin Trans. 1* **1993**, 7, 867–870.
27. Murugesan, N.; Gu, Z.; Stein, P. D.; Bisaha, S.; Spergel, S.; Girotra, R.; Lee, V. G.; Lloyd, J.; Misra, R. N.; Schmidt, J.; Mathur, A.; Stratton, L.; Kelly, Y. F.; Bird, E.; Waldron, T.; Liu, E. C.-K.; Zhang, R.; Lee, H.; Serafino, R.; Abboa-Offei, B.; Mathers, P.; Giancarli, M.; Seymour, A. A.; Webb, M. L.; Moreland, S.; Barrish, J. C.; Hunt, J. T. *J. Med. Chem.* **1998**, 41, 5198–5218.
28. Hewawasam, P.; Meanwell, N. A. *Tetrahedron Lett.* **1994**, 35, 7303–7306.
29. Muchowski, J. M.; Venuti, M. C. *J. Org. Chem.* **1980**, 45, 4798–4801.
30. Strazzolini, P.; Melloni, T.; Giumanini, A. G. *Tetrahedron* **2001**, 57, 9033–9043.
31. He, J. X.; Cody, W. L.; Doherty, A. M. *J. Org. Chem.* **1995**, 60, 8262–8266.
32. Fürstner, A.; Leitner, A.; Méndez, M.; Krause, H. *J. Am. Chem. Soc.* **2002**, 124, 13856–13863.
33. Guo, L.; Bradshaw, J. D.; McConville, D. B.; Tessier, C. A.; Youngs, W. J. *Organometallics* **1997**, 16, 1685–1692.
34. Guo, L.; Bradshaw, J. D.; Tessier, C. A.; Youngs, W. J. *Organometallics* **1995**, 14, 586–588.
35. Youngs, W. J.; Tessier, C. A.; Bradshaw, J. D. *Chem. Rev.* **1999**, 99, 3153–3180.
36. Sengupta, P.; Zhang, H.; Son, D. Y. *Inorg. Chem.* **2004**, 43, 1828–1830.

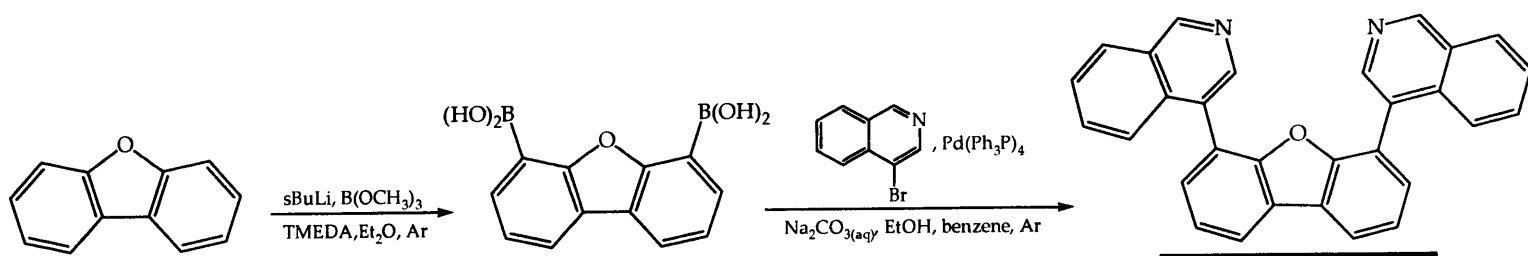


Scheme 3.1.

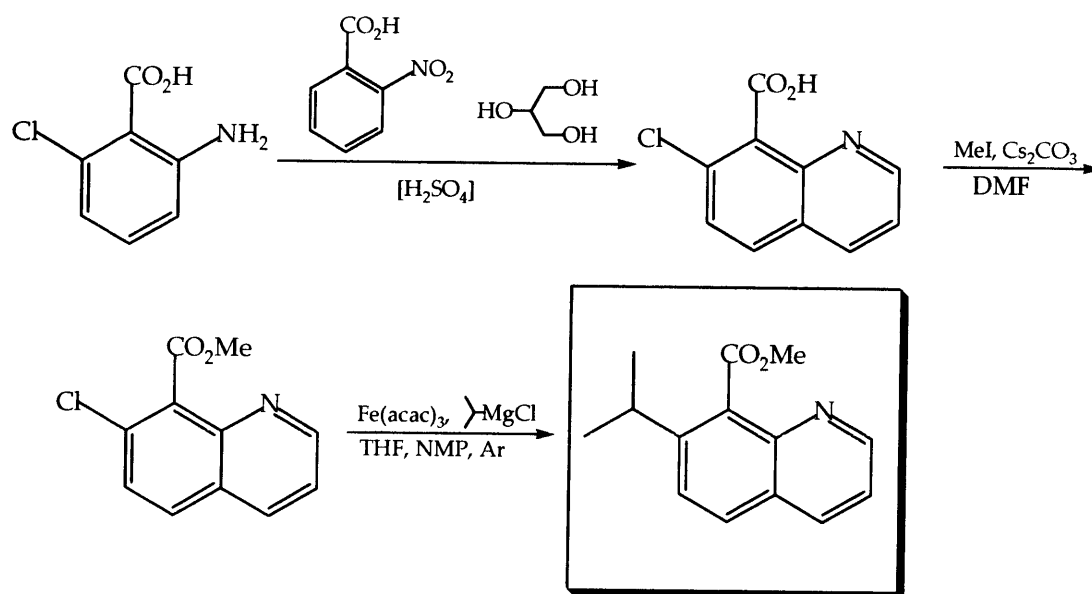




Scheme 3.2.



Scheme 3.3.



Scheme 3.4.

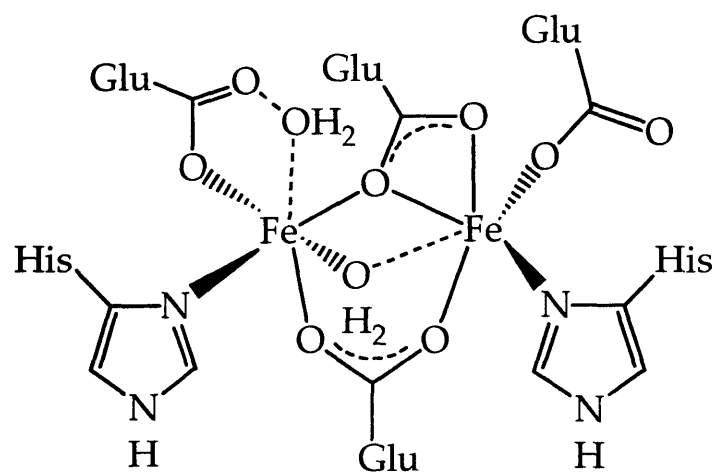


**Figure 3.1.** Detailed representation of the active site of sMMOH<sub>red</sub>.

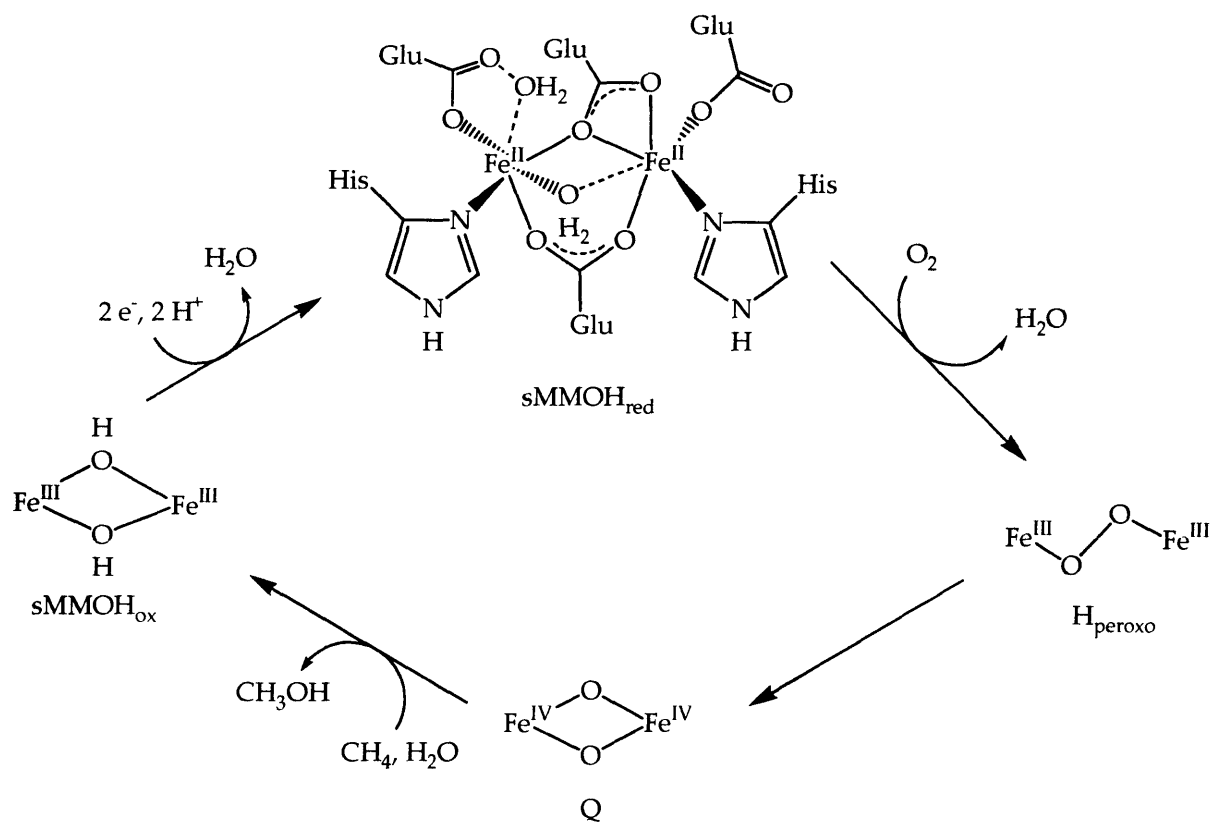


**Figure 3.2.** Proposed catalytic reaction cycle with only spectroscopically visible species.

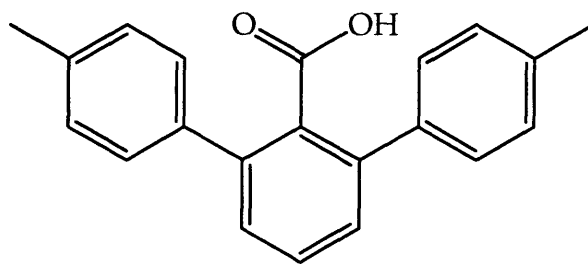


**Figure 3.3.** Example of a sterically hindered carboxylic acid, 2,6-di(*p*-tolyl)benzoic acid ( $\text{Ar}^{\text{Tot}}\text{CO}_2\text{H}$ ).

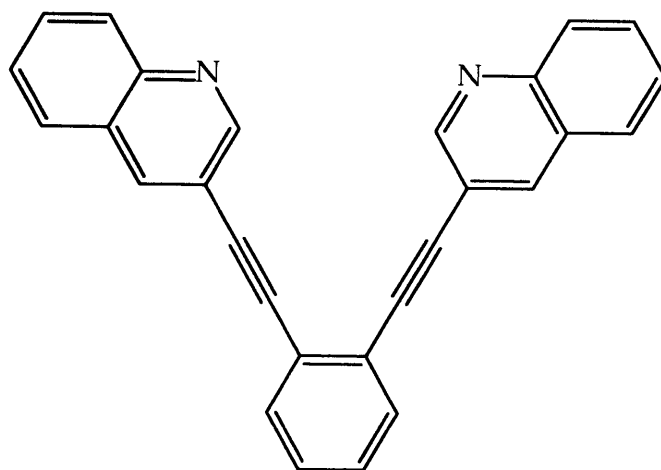


**Figure 3.4.** Representation of BQEB.

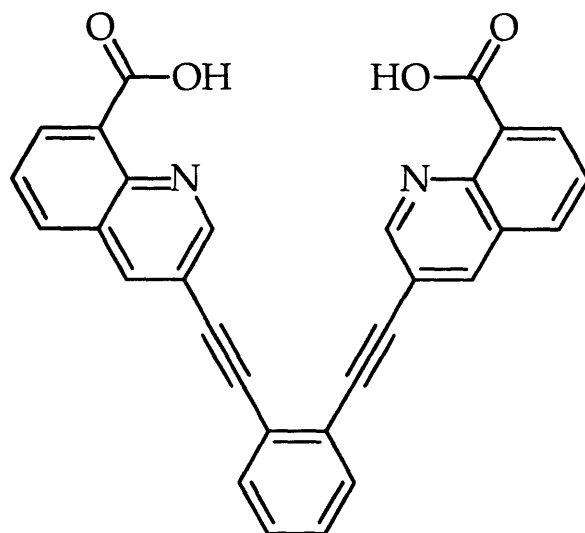


**Figure 3.5.** Representation of H<sub>2</sub>BCQEB.



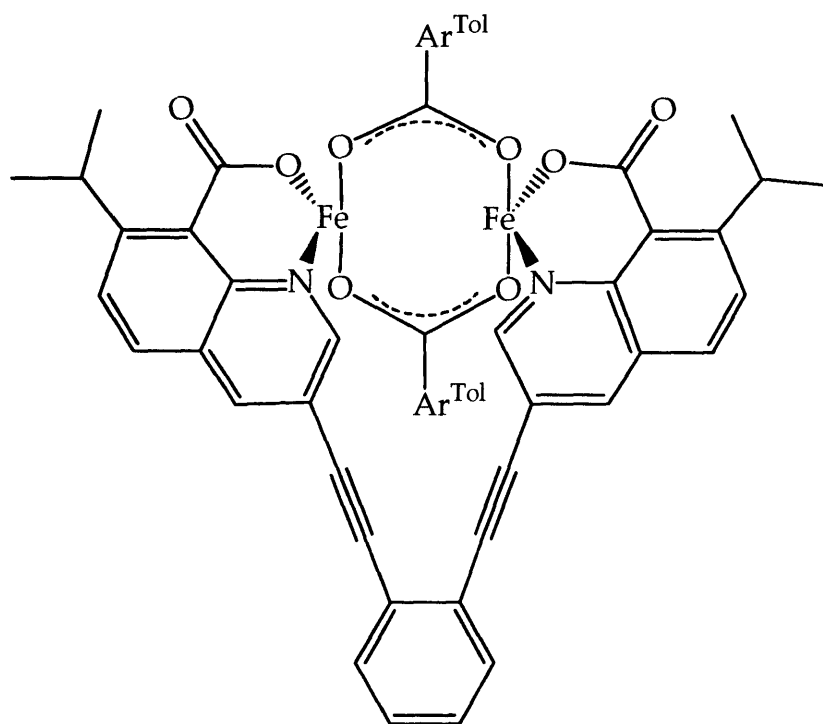
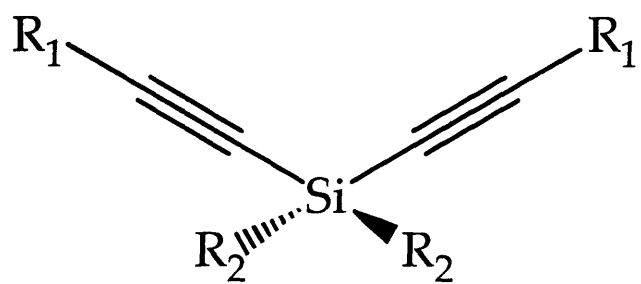


**Figure 3.6.** Desired final diferrous product.



R<sub>1</sub> = pyridine, quinoline

R<sub>2</sub> = Ph, <sup>t</sup>Bu

**Figure 3.7.** General representation of synthesized silanes.

**Biographical Note**

The author was born on July 29, 1980 in Washington D.C. She received her B.S. in Chemistry and Geochemistry from the California Institute of Technology in 2002. Upon completion of her graduate work under Dr. Lippard, she will pursue a Ph.D. in Geochemistry at the Massachusetts Institute of Technology, where she has accepted a Linden Earth System Graduate Fellowship.

**Education****Amy E. Kelly**Masters Chemistry  
2002-2004Massachusetts Institute of Technology  
Advisor: Professor Stephen J. LippardB.S. Chemistry and Geochemistry  
1998-2002

California Institute of Technology

**Publications**Yoon, S.; Kelly, A. E.; Lippard, S. J. *Polyhedron* **2004**, in press.Kelly, A. E.; Macgregor, S. A.; Willis, A. C.; Nelson J. H.; Wenger, E. *Inorg. Chim. Acta*  
**2003**, 352, 79–97.